

**Mobile and Indoor
Antennas for
Digital Television**

Submitted by Luke Shuley

For the Bachelor of Engineering (Honours) requirement in the division of

Electrical and Electronic Engineering

at

The University of Queensland

**Department of Computer Science and Electrical
Engineering (CSEE)**

October 1999

118 Fort Road,
Oxley, QLD 4075
Tel: (07) 3375 5858

The Executive Dean,
School of Engineering
The University of Queensland,
St. Lucia, QLD 4072

Dear Sir,

In accordance with the requirements of the Bachelor of Electrical and Electronic Engineering (honours) degree, I hereby present my final year thesis entitled “Mobile and Indoor Antennas for Use with Digital Television”, supervised by A/Prof. Marek. E. Bialkowski.

I certify that the writings contained within is entirely original work and that any text which is not has been neither misquoted nor attributed inappropriately. I also declare that this thesis has not been previously submitted for assessment.

Yours sincerely,

Luke Shuley.

Acknowledgements

The author of the thesis contained within would like to thank his supervisor A/Prof. Marek E. Bialkowski for his expertise and recommendations for the development of this thesis. Dr. Mikhail Cherniakov also has provided additional backup expertise during the months when A/Prof. Bialkowski was overseas. Mr. Alex Rakic has provided any assistance with antenna measurements and materials procurement.

I would also particularly like to extend my thanks to the mechanical and electrical workshop staff, and especially Keith Lane, whose exceptional craftsmanship have made the realisation of the antenna prototypes a greatly simplified task.

For his unconditional support and limitless advice in the procurement of this thesis, I would like to thank my father, A/Prof. Nicholas Shuley of RMIT University.

Finally a big thank-you to my family and friends, who have provided much support and source of alternative activity during the year.

Abstract

Digital Television is an exciting new area of recent but not yet fully implemented technological development in Australia. A fundamental requirement for Digital Television is the necessity for new antennas for a specific UHF band. Thus, an interest has been recently renewed in the common analogue television antenna. Preliminary research has also indicated that gaps in current antenna technologies exist with regard to Digital Television. Subsequent revisitation of these designs has led to the study of more intricate antennas for different television reception applications, namely the mobile and indoor antenna designs.

The following thesis provides a detailed analysis of two such antenna designs for specific usage in the Digital Television industry. A comprehensive discussion of basic theory and design guidelines as well as processes involved in the numerical computation of current distributions has been performed. Computer-aided design of the wire antennas using *EAM:NEC* has then been conducted with several design iterations leading to the implementation of two final prototypes. Measurements of both these prototypes have indicated that a high degree of theoretical and experimental correlation is evident. Although it has been shown that a majority of the design specifications for both designs have been met, further improvements have been suggested which could lead to the development more accurate designs.

Table of Contents

Acknowledgements	iii
Abstract	iv
List of Figures	vii
Chapter One – Introduction	1
1.0 Origins of Analogue Television	1
1.1 Digital TV development: A Perspective	2
1.1.1 Digital versus Analogue signal formats	3
1.2 Signal Processing of TV signals	3
1.3 Progress of Digital TV in Australia	4
1.4 Some planning criteria for DTV transmission/reception.....	5
1.4.1 Transmission bands.....	5
1.4.2 Polarisation	6
1.4.3 Characteristic impedance.....	6
1.4.4 Notional receiver specifications.....	7
1.5 The Scope of this thesis	8
Chapter Two – Literature Review	10
Chapter Three – Antenna Design Theory	13
3.1 The Yagi-Uda Array of linear elements	14
3.2 Planar Reflectors	18
3.3 Integral Equation Method	19
3.3.1 Finite Geometry wires.....	20
3.3.2 Development of Pocklington’s Integral Equation.....	21
3.4 Method of Moments Solution	23
Chapter Four – Computer Analysis and Design	27
4.1 Antenna Design Software	27
4.2 Indoor Antenna Simulation.....	29
4.2.1 Design Iteration One (yagi_d1.nec).....	31
4.2.2 Design Iteration Two (yagi_d2.nec)	33
4.2.3 Design Iteration Three (yagi_d3.nec)	34

4.3 Design of Feed Network for Modified Yagi.....	36
4.4 Indoor antenna – Mechanical Design	37
4.5 Mobile Antenna Simulation.....	39
4.5.1 Design Iteration One (h_rhomb.nec)	40
4.5.2 Design Iteration Two (spider1.nec) – Wideband design.....	40
4.5.3 Design Iteration Three (spider2.nec)	42
4.6 Mobile Antenna – Mechanical Design	44
Chapter Five – Measurements	47
5.1 Measurement Setup	47
5.2 Gain Calculation using Numerical Integration	48
5.3 Dipole Transmitter Antenna	50
5.4 Measured Results	51
5.4.1 Indoor Antenna Prototype	52
5.4.2 Mobile Antenna Prototype	55
Chapter Six – Conclusions	58
Bibliography	60
Appendix A – AutoCAD of final Antenna Prototypes	62
A.1. Indoor antenna: Sheet 1 of 2 – Mechanical Dimensions	63
Sheet 2 of 2 – Electrical Dimensions	
A.2. Mobile antenna: Sheet 1 of 1 – Electrical Dimensions.....	64
Photographs of Antenna Prototypes	65
Appendix B – Software Listings	67
B.1. EAM:NEC input and output file structure	68
B.2. MATLAB programs.....	70
Appendix C – Simulation Data	73
C.1. Indoor antenna radiation patterns and current distributions.....	74
C.2. Mobile antenna radiation patterns and current distributions.....	75
Appendix D – Measured Data.....	76
D.1. Indoor antenna – Return loss and Radiation patterns	77
D.2. Mobile antenna – Return loss	78

List of Figures

Table 1.0	: Frequency allocation for DCP	6
Figure 1.1	: Digital Video Broadcasting on a Singapore bus.....	8
Figure 3.0	: Two-element array of half-wave resonant dipoles showing an endfire radiation pattern	16
Figure 3.1	: (a) Radiation pattern characteristics of increasing reflector length (b) Radiation pattern characteristics of decreasing director length	16
Figure 3.2	: Three-element Yagi-Uda array, formed by incorporating the results of Figure 3.1(a) and (b)	17
Figure 3.3	: General configuration for Yagi antenna with arbitrary number of directors	18
Figure 3.4	: Corner reflector configuration for the Yagi-Uda antenna.....	19
Figure 3.5	: Uniform Plane wave incident on a conducting piece of wire.....	21
Figure 3.6	: Wire segmentation of dipole showing the equivalent current (a) on the surface and; (b) along the centre	26
Figure 4.1	: Dipole antenna behaviour with $L=1.0\text{m}$ and $a= 0.0016\text{m}$	29
Figure 4.2	: Return loss vs. frequency for yagi_d1.out.....	32
Figure 4.3	: Return loss vs. frequency for yagi_d2.out.....	33
Figure 4.4	: Radiation Patterns for final indoor antenna prototype	35
Figure 4.5	: Current Distribution for yagi_d3.nec	35
Figure 4.6	: Impedance Plot of all three modified Yagi-Uda designs	36
Figure 4.7	: The Bazooka balun.....	37
Figure 4.8	: General configuration for mobile antenna.....	39
Figure 4.9	: h_f parameter sensitivity analysis	41
Figure 4.10	: Radiation patterns for final indoor antenna prototype	42
Figure 4.11	: Current distribution for spider2.nec	43
Figure 4.12	: Comparison of the return loss for all three Mobile antenna designs ..	44
Figure 4.13	: Dipole transmit antenna (side view configuration).....	45
Figure 5.0	: Measurement setup within far-field anechoic testing facility	48
Figure 5.1	: Return loss of transmitter	51
Figure 5.2	: Comparison of return loss to simulated data of yagi_d3.nec	52

Figure 5.3 : Measured azimuth radiation pattern for yagi_d3.nec.....	54
Figure 5.4 : Comparison of return loss measurements to simulated data of spider2.nec.....	56
Figure 5.5 : Elevation Pattern for spider2.nec (experimental)	57
Figure 5.6 : Azimuth Pattern for spider2.nec (experimental)	57

Chapter 1

Introduction

Chapter 1 introduces the topic of digital television (DTV) and gives a short background of the developments to date. The background progress is briefly discussed in section 1.1. The Australian implications of the new *Digital Terrestrial Television Broadcasting* standard for DTV or **DTTB-DTV** are studied in section 1.3 and are based on the relatively high quality standards justified in section 1.2. The chapter ends with a concise discussion on the specifications of the antennas to be used for DTV reception for both the stationary and mobile receiver configurations.

1.0 Origins of Analogue Television

The first standardised television set available for consumers originated in North America in 1942, more than half a century ago. By the year 1949, the television communications (telecommunications) industry was a vigorously and rapidly growing sector of both commerce and technology, with television receiver sales averaging to more than 10,000 per month! What role television played for the general public in this time period is essentially the same as what people view it as today, i.e. an information source predominantly for broadcasting of news, sport and entertainment.

It would be reasonable to say that the standard of television and its associated services have essentially remained unchanged, thus withstanding a long period of swift technological change. It is therefore perhaps a remarkable feat that today's television receiver is still capable of receiving the same signals format which was decided upon some fifty years ago.

The accelerating technology advancements in analogue television systems have both created many great benefits to international business markets and spawned growth and

development in the consumer electronics industry. In spite of the numerous benefits, up until now, there has not been sufficient impetus to move to more sophisticated technologies. Thus causing television receiver sets to become increasingly sophisticated, reliable, inexpensive, etc. without the implied shift to a new standard.

With the arrival of Digital Television (DTV), the present equilibrium of analogue television standards has been severely disturbed due to an entire renewal of analogue television technology. The significant advantages and the “door-opening possibilities” of DTV heavily outweigh the previous analogue system, thus warranting such a severe change.

1.1 Digital TV development: A Perspective

Colossal investments have been made into research and development of DTV systems to a point where disruptions on market and business levels have occurred. All in an effort to obtain notable advantages associated with a broader applications base as with DTV systems. Coupled with computer applications, DTV will allow services such as video conferencing, Internet access and multimedia productions. Some of these services have already been technologically developed for DTV systems and will shortly be available on the market.

Compared to the analogue television systems, digital systems offer several important advantages (elaborated upon in the next section). Consequently, over the last thirty odd years, countless electrical appliances and electronic equipment have progressed in functionality and/or improved with the shift into the digital realm.

The future of Digital television is heading for multi-integrated systems between all forms of communications allowing personal computing in consumer television and access to Internet and other domestic services.

1.1.1 Digital versus Analogue signal formats

One of the most important advantages of a digital signal over an analogue signal is its relative immunity to noise in signal transmission. Noise in analogue stages is additive, causing various transmitter and receiver sub-systems to contribute noise to the overall signal, thus causing the noise level to be greater than the worst stage in the analogue system. Relative measurements of signal and noise strength commonly known as the *signal-to-noise ratio* (SNR) in analogue systems exhibit what is called “graceful degradation” [15].

With the use of the digital signal format, multiple generative recordings and production of TV programs with complex editing functions can be achieved with little or no corruption of the SNR. This is one of the major reasons why digital recording equipment is used exclusively.

Digital signal formats also exhibit smaller effects of SNR degradation due to bit errors in serial bit-data. However, these can be easily corrected with error correction circuits provided the BERs (Bit Error Rate) are not too high. One significant drawback however, with the use of digital signal transmission in broadcasting, is that a point is reached where beyond which the SNR drops to a level that warrants favourable use of analogue transmission. This implies that reception of digital television signals in rural or outback areas; long distances from broadcast towers could/would have marginal signal strengths. Providing high gain antennas for DTV reception in these circumstances would significantly improve the digital signal strengths and thus avoiding the need for increased numbers of DTV transmission stations.

1.2 Signal Processing of TV signals

According to the Nyquist criterion, the frequency bandwidths of digital signals are considerably greater than that of their analogue counterparts. The bandwidths are also further increased to allow for bit error correction algorithms, leading to (in some cases) a factor of $\sim x10$ greater bandwidth required for DTV signals. This phenomenon leads extremely low spectral efficiency.

DTV signal equivalent frequency bandwidth is a rather important concept. Obviously, in order to justify implementation of digital television, one must seriously consider the need of bandwidth reduction processes so that more efficient use of the allotted frequency spectrum.

Frequency bandwidth compression techniques that are able to efficiently compact the digital signal into a similar bandwidth occupied by a corresponding analogue signal are currently being developed and refined for further improvement. For example “Bandwidth Compression” algorithms such as the international standard, CCIR-601 TV (developed by the International Radio Consultative Committee [1]) has the capability of sampling and interchanging a 216Mb/s digital bit-sequence for a 6-8MHz analog channel! The implication of this is that the same channel allocations as the current analog system can be used, thus partly providing for the reception of digital signals on present receivers.¹

Digital Compression is one of the essential issues and probably the most important technological concept in making it possible to replace analogue TV with DTV. Digital compression techniques already have generated much excitement and potential for development both in the Engineering and television industries. Systems have currently been proposed where compression ratios up to 100:1 are going to be implemented!

1.3 Progress of Digital TV in Australia

In order to implement a television broadcasting system many different technical factors need to be taken into account and the resulting system is subsequently quite a demanding engineering challenge.

The Australian Broadcasting Authority (ABA) has produced a number of guidelines and planning directions for the implementation for a Digital Television system in Australia. As suggested in [1], the most suitable broadcasting method for Australia is DTTB-DTV. The planning criteria have been based on recommendations and reports

¹ This same philosophy was used in the Black and White conversion to Colour in Australia in 1975

published by the ITU (International Telecommunication Union). Standards Australia has also played an important role as the body ultimately responsible for developing and publishing technical parameters used for transmission and reception of digital television signals.

The major guidelines and planning criteria as produced by the ABA for a national DTTB and Digital Channel Plan can be described in section 1.3.1.

1.4 Some planning criteria for DTV transmission/reception

From technical reports and planning recommendations by the ITU, it has been decided by the ABA in conjunction with the Digital Television Channel Planning Consultative Group to adopt a DTTB system. DTTB would allow hybrid transmission of:

- 1. Substantially uncompressed 525/625 line component video;**
- 2. Compressed multi-program video;**
- 3. High Definition (HDTV) video; and**
- 4. Standard Definition Television (SDTV) to portable and mobile users.**

The Digital Television Channel Planning Consultative Group has completed drafts for a *Digital Channel Plan* (DCP) and a proposal for frequency allotment to the Australian Television Frequency Spectrum has been implemented in [1].

1.4.1 Transmission bands

For implementation of the DCP, it has been decided that channel selection will occur from those 7-MHz channels occupying transmission bands III, IV and V of the TV frequency spectrum allotment shown in table 1.0.

TV transmission band	Frequency Range (MHz)	Channels
III	174 – 230	VHF Channels 6-12
IV	526 – 582	UHF Channels 28-35
V	582 – 820	UHF Channels 36-69

Table 1.0 - Frequency allocation for DCP [1]

Some of these channels are the same as previously used for national analogue transmission, and can be reused in view of digital compression techniques. Channel frequency spacing, which is normally used in analogue or hybrid (Digital-Analogue) TV systems to improve compatibility between adjacent channels, will not be considered in this all-digital channel plan.

1.4.2 Polarisation

Similar to analogue TV signal standards, polarisation of the DCP television services has been chosen to be horizontal. Both transmission stations and receiver antennas are therefore required to adopt this standard.

1.4.3 Characteristic Impedance

As with most coaxial cables for regular television applications, the standard characteristic impedance used is $Z_o = 300\Omega$. However, for practical measurement purposes (which will be covered in later chapters) of this thesis project, a characteristic impedance of $Z_o = 50\Omega$ is selected.

1.4.4 Notional receiver specifications

As the title of this thesis suggests, the ultimate aims are to conceive two antenna designs for use with the proposed DTTB system in Australia. Two particularly useful receiver antennas that will be discussed exclusively are for the applications of mobile and indoor DTV reception. A comprehensive discussion leading to the development of the requirements for both the antennas will be now performed.

Firstly, the indoor antenna must be designed so that it will be able to be placed inside the roof cavity of a medium sized house. Therefore, a size limit must be placed on the indoor DTV antenna design. The antenna shall be stationary and so a directivity as high as possible is desired. Gain levels of the antenna should be as large as possible in order to receive the minimum signal strengths (gain is directly related to directivity). The bandwidth must be sufficiently large to accommodate all of the television channels in the number IV TV transmission band mentioned in the planning criteria. Justifications for choosing this band are due mainly to constrictions imposed by UQ measurement facilities (also reviewed in chapter five: measurements). The antenna testing range to be used for this study is a high-frequency range and unsuitable for very low frequencies, hence band III is eliminated. Band V is eliminated on grounds that the bandwidth is much too large for a resonant antenna and a very wideband design would need to be implemented. Note that only resonant antenna structures, which do not allow implementation of wideband designs, are being contemplated in this thesis. Transmission band IV is therefore the most suitable band for the design of both antenna designs.

A more interesting and recent application is the mobile TV antenna receiver, which can be easily positioned on the roofs of cars, buses, trains etc. On the following page is evidence of DTV services, already employed by transportation companies. Other DTV applications, particularly prevalent on public transport are the use electronic posters for advertising purposes. This new form of advertising is a low maintenance and cost-effective as well as an “eye-catching” method for endorsing products.



Figure 1.1. Digital Video Broadcasting on a Singapore bus [2]

The mobile antenna specification requires most importantly, the correct radiation pattern. As with most types of mobile receiver antennas, the radiation pattern must be an omni-directional pattern in order to receive signals from directions according to the motion of the vehicle. It is also simultaneously desired for the mobile antenna to possess a relatively large gain as with the indoor antenna (This requirement is assisted with the use of a ground plane). Thirdly, a similar bandwidth to the indoor antenna is also desired so that the mobile antenna can receive similar DTV channels. Another possible feature is the addition of a dielectric radome to protect the device from the elements.

1.5 The Scope of this thesis

Based on consideration of the preliminary specifications and brief review of various wire antennas, the two most popular candidates for the implementation of the two antennas are:

1. For the indoor case: **Choose a modified Yagi-Uda array of linear elements.** Modifications must be made to the antenna in order to improve the gain, increase the frequency bandwidth and to decrease the size of the antenna.

2. For the mobile case: **Choose a modified Folded Dipole Array.** The general dipole is chosen because of its simplicity. An array is formed so as to improve the gain and obtain an omni-directional field pattern. However this design is only an initial guideline and may change form at a later stage in this thesis.

In view of the ABA proposal for DTTB in Australia, the main aims/goals of this thesis have been carefully chosen to be:

1. Develop designs for both the mobile and indoor antennas using a wire antenna computer aided design package.
2. Construct both the antennas and conduct measurements on a far-field test range facility.
3. Correlate the design and prototype. Ensure that the antennas discussed meet all (or a majority of) the design specifications.
4. Suggest means for future applications and possible improvements on design for further (or more advanced) specifications.

Chapter 2

Literature Review

As stated previously, there are two different antenna designs that need to be designed and constructed. The first, is a modified version of the Yagi-Uda antenna, while the second may be regarded as a modified array of folded dipoles extended into “rhombic-shape” loops. Although the Yagi-Uda antenna has considerable design coverage in the literature, the mobile antenna (as we shall see in subsequent chapters) has only limited theory and essentially constitutes a new design. For this reason much of or (even all of) the theory covered in this chapter relates mainly to the Yagi-Uda antenna.

The literature review is broadly split into three different sections based on the scope of the thesis. The articles reviewed include those related to basic wire antenna theory and design, computer analysis methodology (method of moments or similar) and specialised theory relating to specific aspects of wire antenna design (eg. optimisation of specific parameters). We now review these three sections.

Constantine A. Balanis [3] has provided much of the basic antenna theory needed to develop the modified Yagi-Uda antenna design. In particular, a comprehensive discussion of the operation of Yagi-Uda antenna is provided. Similarly, an antenna design procedure and subsequent calculation of the current distribution using the Method of Moments (MoM) are both incorporated. Again in [4], the basic principles of radiation applied to the Yagi-Uda antenna; but this time by using an intuitive coupling explanation. A particularly useful parameter study that can be used for design purposes for the Yagi-Uda together with a useful design example is also provided in [4]. Kraus [5] also mentions some of the theory associated with the various modifications made to the Yagi-Uda antenna. As will be evident in later chapters, [5] has been essential in the design of the mesh reflector in the Yagi design.

With regards to the computer analysis methodology, Mitra [6] covers much of the necessary antenna theory and analysis. This begins with an integral equation formulation and then uses the MoM. MoM is essentially a procedure to reduce the integral equation to a matrix equation. The procedure is mainly numerically based and requires knowledge of numerical integration techniques in order to compute the entries of the matrix. The main object is to obtain the (exact, or a close approximation to) the current distribution on the antenna. Once this is found, all the related parameters may be found from direct analytical formulas. The latter half of chapter three will describe some of the equations and theory utilised in MoM.

More complex journal articles related to specific aspects of the Yagi-Uda were found in the Antenna and Propagation Transactions. These have proven to be useful alternatives to the above mentioned references. Although some of the articles have proven to be far too specific for the nature of this thesis, nonetheless two papers were sufficiently interesting to note briefly here.

The article [7] presented by Shen demonstrates an interesting optimisation gain/directivity-bandwidth procedure for use with Yagi-Uda arrays. Theoretically, Shen describes the numerical analysis of wave propagation on a periodic linear infinite structure. A travelling wave is supported on this structure which introduces several modes and associated “pass-bands” on the ω - β dispersion characteristic. This indicates that multiple modes can coexist which is a potentially interesting application for DTV antennas requiring multiple-band TV reception.

A paper on methods developed for maximisation of the forward directivity of Yagi-Uda arrays is covered in [8]. A complete set of geometrical parameters is taken into account in the study including design examples for various size Yagi-Uda arrays. The method used comprised a MoM procedure coupled with a perturbation technique to calculate the optimum parameters.

The DTV proposal published by the ABA [1] has presented a complete and concise summary of the benefits to the Australian Public in choosing a DTTB-DVB standard for the purpose of digital Television. The 28-page report discusses some of the

important requirements of the DTV standard involving technical specifications. On page 4 of this document, a Digital Channel (frequency allotment) Plan (DCP) for the DTTB-DVB Australian standard is introduced. The DCP is subsequently created as one of the more important motivations for this thesis. Another of the more important aspects of this report is that it provides extremely useful notional receiver specifications for the Digital Channel Plan. In summary, this proposal has been utilised exclusively to create the much of the specification list for both of the antenna designs mentioned in chapter one.

Chapter 3

Antenna Design Theory

It was mentioned in chapter two that the mobile antenna has limited associated design theory compared to that of the indoor antenna design. Although much antenna theory exists on folded dipole antennas, limited design procedures were available for this type of resonant structure. It is also speculated that the mobile design structure will vary significantly from the general folded dipole geometry.

Therefore in view of the above, the aim of this chapter is to address the relevant theory required for the principles of operation of the Yagi-Uda design (§ 3.1). Section 3.1 will specifically discuss the modeling of the Yagi by looking at an intuitive understanding of the Yagi antenna and use these concepts as a basic model for more sophisticated formulation; namely the MoM. In addition to the Yagi, some design guidelines for the mobile antenna will be provided in § 3.3. The integral equation, being the basis for MoM, is regarded as the best alternative that will allow us full design flexibility. Although new MoM program code will not be presented in this thesis, information to allow the user better control over a computer package that uses MoM as it's solution environment will be emphasised. The antenna simulation software, EAM: NEC or *Electromagnetic Antenna Modeling System using Numerical Electromagnetic Code* [9] was used in this thesis and will be further discussed in chapter 4.

As Mentioned in preceding chapters, there are different requirements for both the indoor and mobile antenna. Although both antennas are to receive over a similar specified band of frequencies, the required radiation patterns are quite different. The indoor antenna will be always pointing towards the transmitter and should thus possess a relatively high directivity, whereas the mobile antenna should be capable of receiving from any direction leading to the requirement of an omni-directional

pattern. Bearing in mind that the Yagi-Uda antenna has served well in the reception of analog TV signals, we ask whether a similar version of the same antenna may be used for the DTV case. We will thus investigate the Yagi-Uda as our primary antenna of choice for the DTV application.

Mobile TV reception however, is a more recently developed concept and investigations to improve some of the design parameters of current antennas for the receiver will be performed. An existing popular type of mobile receiver [12] features a V-type antenna reflected in a ground plane to create the omni-directional pattern.

As mentioned previously, the most important requirement for the mobile TV/DTV antenna is that an omnidirectional radiation pattern is utilised to allow reception of signals from all directions. Exploration into the possibility of using an array of extended folded dipole antennas into a rhombic-shape² antenna to improve some of the parameters of the V-type antenna will be carried out.

3.1 The Yagi-Uda Array of linear elements

Both professors Shintaro Uda and colleague H.Yagi of the Tohoku Imperial University, Sendai Japan first described the operating principles of the radiator in 1926 [10]. Today it is known as the Yagi-Uda array of linear elements or simply the Yagi. Although the Yagi-Uda is commonly classified as a single antenna, it is in fact an array of antenna elements. This fact will assist in the discussion of optimisation in chapter 4. The array is a so-called *parasitic* array as it only contains one linear element that is excited as the *feed*. The other elements of the array are therefore parasitically fed by the driven element that near field couples electromagnetically to the other elements of the array - *the directors*. Relatively high gain levels are possible due to the arraying technique but since the array is only fed at one position, increased gain cannot always be achieved by simply adding more directors. There is a ‘law of diminishing returns’ in gain enhancement using this method. Primarily the parasitic effect is a simple method of achieving high gain. Since only one element is excited,

² Not to be confused with a “Rhombic antenna”: a wideband travelling wave type design

the cost is minimal. This is no doubt one of the prime reasons why the Yagi has endured as the main antenna of choice for analog television for so long.

The basic operation of the Yagi-Uda array from a first-principles point of view is a particularly effective method for understanding the function of the antenna. This method has been effectively demonstrated in [4] and will therefore be presented in this section. The basic format of the Yagi-Uda array consists of three elements, one driven element, one director and one reflector, i.e. two elements are parasitic. We construct a three element Yagi-Uda by first adding one parasitic element adjacent to the driven element. An electric current is induced in the parasite and subsequently a secondary radiating field is generated by the parasitic element with a field roughly the same as the field generated by the driver.

$$E_{incident} = E_{driver} \quad (3-1)$$

Now since the total tangential component of the electric field on any perfect conductor is zero, then it can therefore be concluded that the sum of the tangential components of the incident field on the parasite and the driver is zero. This means that the field radiated by the parasite and that radiated by the driven element are equal and opposite in phase. Combining this fact and equation (3-1) we get:

$$E_{parasite} = -E_{incident} = E_{driver} \quad (3-2)$$

Ordinary array theory tells us that two closely spaced, equal amplitude, oppositely phased elements will radiate in the endfire direction [3]. The driven element will be normally be resonant with length slightly less than $\lambda/2$ (normally 0.45λ - 0.49λ), where λ is the free space wavelength of the desired signal to be received by the antenna. The radiation pattern generated from the array of the combination of these two elements will be (as noted above) in the endfire direction as shown in Figure 3.0.

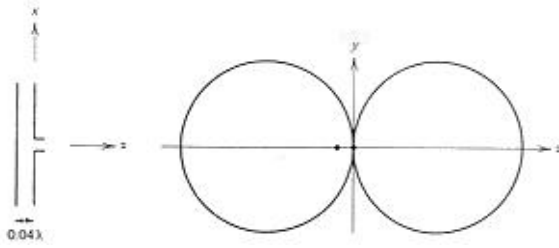


Figure 3.0. Two-element array of halfwave resonant dipoles showing an endfire radiation pattern [4].

By now varying the length of the parasitic element, alteration of the beam shape is possible in order to obtain a slightly more directive pattern. Typical director lengths will therefore be slightly *shorter* than the driven element. Similarly, the third element of the array - the *reflector* is normally longer than the driven element and has the net effect of reflecting the radiation from the driver, thus again increasing the directivity of the pattern. Effects on the radiation pattern due to an increased reflector length is shown in Figure 3.1a, while the effects of a decreased director length are shown in Figure 3.1b.

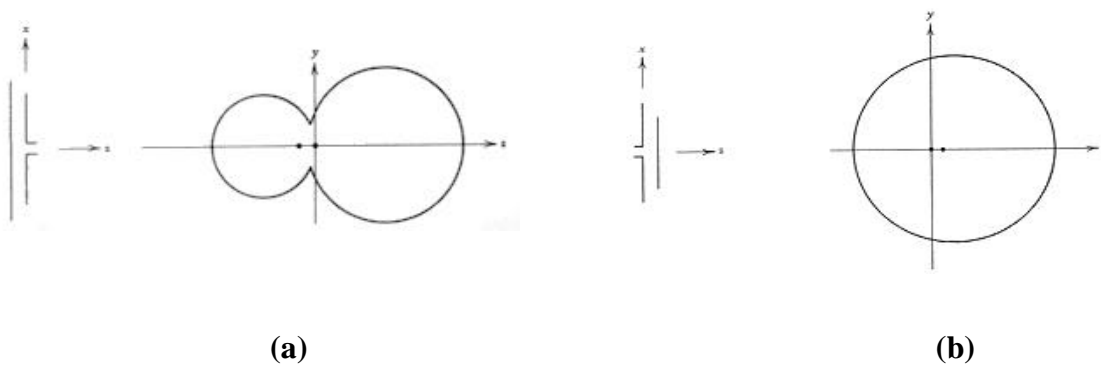


Figure 3.1 (a) Radiation pattern characteristics of increasing reflector length; and (b) Radiation pattern characteristics of decreasing director length

Taking the analysis one step further and combining the two different array geometries, it is possible to achieve significant beam formation. Figure 3.2 illustrates the improvement made on the radiation pattern by combining the director and the

reflector patterns to that of the driven half-wave dipole. By subsequently adding additional directors to the array, larger gain levels in the forward direction can be obtained. However the relationship between the number of elements and the gain is non-linear, and a point is reached where additional elements (directors) will only provide minimal improvements to the gain and only increase the size of the antenna unnecessarily.

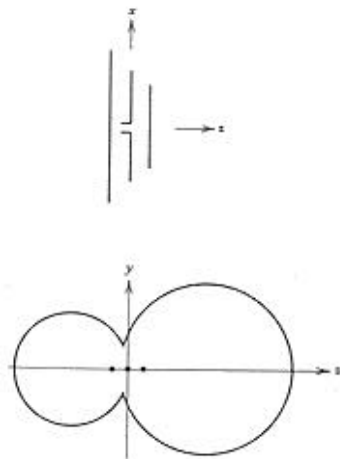


Figure 3.2. *Three-element Yagi-Uda array, formed by incorporating the results of Figures 3.1(a) and (b).*

The general configuration of all the different Yagi antenna geometry parameters are shown in Figure 3.3. The parameters are:

L_R : length of reflector.

L : length of driven element

L_D : length of directors

S_D : Spacing of directors

S_R : spacing of reflector from driven element

N : number of directors.

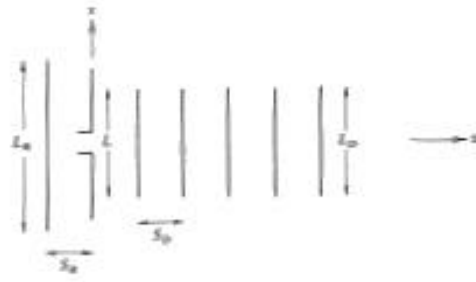


Figure 3.3. General configuration for Yagi antenna with arbitrary number of directors [4].

It is to be noted that in the above diagram, the all directors are considered to be of equal length and are equally spaced. Furthermore, it is also assumed that the wire radii of all elements are the same. In a model capable of changing all these parameters independently, it may be possible that the optimum configuration (in some sense) can be reached. The parameter(s) regarded as interesting from an optimisation point of view are impedance bandwidth, E & H plane beamwidths, front-to-back ratio, sidelobe levels and gain.

3.2 Planar reflectors

Another interesting aspect of the Yagi-Uda antenna is the possibility of implementing a planar reflector, an arrangement widely utilised in UHF-band television antennas. Two different major types of planar reflectors applicable to wire antennas, discussed in Kraus [5] are the cylindrical parabolic and corner type reflectors. Kraus has indicated that the type of reflector should be implemented according to effective aperture of the antenna.

Ideally with large apertures ($>2\lambda$), cylindrical parabolic reflector planes should be used where the driven element is a linear wire element. However, for smaller apertures, it is more effective (and simpler) to use planar reflectors for similar gain levels. The size of the antenna is favourably smaller and so it is envisaged that a corner type reflector will be implemented. Figure 3.4 illustrates the general configuration of corner reflectors.

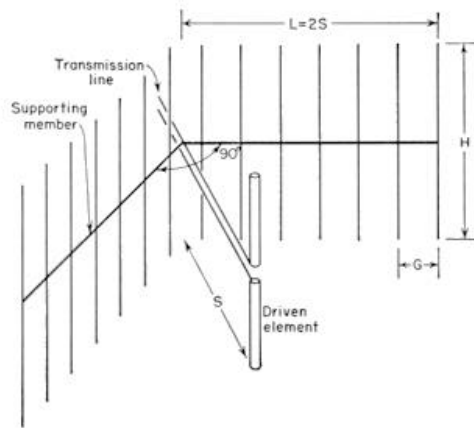


Figure 3.4. Corner reflector configuration for the Yagi-Uda antenna [5].

3.3 Integral Equation Method

As might well be appreciated, the task of predicting the performance of the Yagi-Uda antenna is made difficult by the large number of variables. In fact, perusal of the literature suggests that selection of director lengths and their spacings (for example) has been largely empirical or has been decided by lengthy experimental data [11]. There hence exists a need for a rigorous method of determining the currents on all elements of the antenna. Once these currents have been found, it is a relatively straightforward task of determining the radiation pattern, input impedance and other derived quantities. This section looks at methods for obtaining such a current distribution. The problem of determining the current distribution will be formulated as an integral equation and the task of solving the integral equation will be via the *Method of Moments*. Since the NEC code is essentially a MoM code, we will look at this in some detail.

The electromagnetic analysis of finite geometry wire scattering or radiation is performed by the *Integral Equation (IE)* method. The objective of the IE method is to calculate the unknown charge/current distribution present on the surface of the wire due to some type of excitation (the wire itself acts as either an antenna or a scatterer

depending on type of excitation). The process involves first formulating an integral equation for the unknown current/charge distribution via the boundary conditions thus deriving, in fact, what amounts to a boundary value problem. The equation itself is then usually solved utilising numerical techniques as employed in MoM. For conducting bodies composed of thin wires i.e. Structures composed of interconnected cylinders whose radii are small in terms of wavelength (thin wires) are the main element of the NEC program. To effectively demonstrate the IE method, this thesis will briefly review *Pocklington's integro-differential equation* as being representative of that employed in NEC. Thereafter follows a quantitative description of the MoM.

3.3.1 Finite geometry wires

Evaluating current densities on finite diameter wires is most conveniently calculated using three-dimensional IE techniques as specialised to wires. There is a wide variety of integral equation formulations for wires, all of which are based on the following assumptions [3]:

1. Azimuth or circumferential currents produce negligible effects compared to the axial current along the wire.
2. The induced electric sources on the surfaces of the wires can be located on the axis of the wires, thus giving rise to filamentary source representations.
3. The boundary condition on the electric field can be enforced on the surface of the conductor.

The most common formulations are *Pocklington's integro-differential equation* and *Hallen's integral equation*. Pocklington's equation is the more favourable method of analysis because it is more flexible to different types of feed sources. Hallen's equation only permits delta-gap voltage source models at the wire antenna feeds.

3.3.2 Development of Pocklington's Integral Equation

Assume that an incident wave, with *incident electric field* $E^i(\mathbf{r})$, impinges onto the surface of a conducting piece of wire as shown in Figure 3.5. The incident electric field induces a current density onto the surface of the wire, which subsequently re-

radiates to produce a *scattered electric field*, $E^s(r)$. At any point in space from the wire, the *total electric field* can be considered as the sum of the incident and scattered fields,

$$E^t(r) = E^i(r) + E^s(r) \quad (3-3)$$

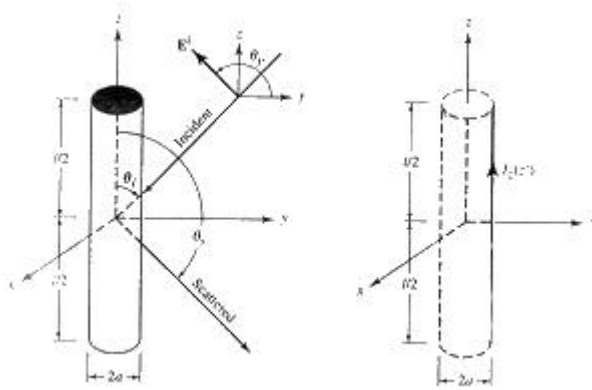


Figure 3.5. Uniform plane wave incident on a conducting piece of wire [3].

If we move the observation point to the surface of the wire, we find that the tangential component of the total electric field vanishes [3]. In cylindrical coordinates, the tangential components of the incident and scattered fields can be equated:

$$E_z^s(r = r_s) = E_z^i(r = r_s) \quad (3-4)$$

The general form for the scattered electric field is:

$$E^s(r) = -j \frac{1}{\omega \mu \epsilon} [k^2 A + \nabla(\nabla \cdot A)] \quad (3-5)$$

The vector potential, A_z of the wire in Figure 3.5 can be described in terms of the current density, J_z :

$$A_z = \frac{\mathbf{m}}{4\mathbf{p}} \int_{-l/2}^{+l/2} \int_0^{2\mathbf{p}} J_z \frac{e^{-jkR}}{R} a d\mathbf{f} dz' \quad (3-6)$$

By now making the assumption that the wire is very thin allowing J_z to be expressed in terms of I_z and not a function of the azimuth, then rearranging equation 3-6:

$$\begin{aligned} A_z &= \mathbf{m} \int_{-l/2}^{+l/2} I_z(z') \left(\frac{1}{2\mathbf{p}} \int_0^{2\mathbf{p}} \frac{e^{-jkR}}{R} d\mathbf{f} \right) dz' \\ &= \mathbf{m} \int_{-l/2}^{+l/2} I_z(z') G(z, z') dz' \end{aligned} \quad (3-7)$$

Which is evaluated at the surface of the conductor, $\rho = a$. Finally the above equation can be substituted in to the z-component of the scattered electric field (described in equation 3-5).

$$E_z^a(\mathbf{r} = a) = -j \frac{1}{\mathbf{w}\mathbf{e}} \left(k^2 + \frac{d^2}{dz^2} \right) \int_{-l/2}^{+l/2} I_z(z') G(z, z') dz' \quad (3-8)$$

Using equation 2-7 and rearranging yields,

$$\int_{-l/2}^{+l/2} I_z(z') \left[\left(\frac{\partial^2}{\partial z^2} + k^2 \right) G(z, z') \right] dz' = -j\mathbf{w}\mathbf{e} E_z^i(\mathbf{r} = a) \quad (3-9)$$

Equation 3-9 is known as *Pocklington's equation*. Notice that the unknown quantity that we wish to determine is the current under the integral sign.

3.4 Method of Moments solution

The MoM concept applied to the numerical treatment of radiation problems is essentially a reduction of the corresponding integral equations adopted in the analysis

to a system of linear algebraic equations. The integral equation of the previous section, or for that matter any integral or differential equation may be expressed in operator form as:

$$Lf = g \tag{3-10}$$

where L is the *linear integro-differential operator* (as in the case of Pocklington's IE equation), g is a known *excitation function* and f represents the unknown response function, in this case the current on the wire.

The method of solving this operator equation is to first approximate the unknown f as a series of so called *basis functions*.

$$f = \sum_{n=1}^N a_n f_n \tag{3-11}$$

Here, f_n are the basis functions which are assumed known and are selected according to the problem at hand. The a_n terms are so far unknown complex coefficients we wish to evaluate. We note that should we know the N a_n terms, then we can immediately write the series solution for the problem. We also note that we have assumed that N terms are sufficient to describe f . This is in general unknown. However, if we increase N sufficiently until the solution does not change, then we have a kind of convergence criteria for f . We will assume that convergence to the correct solution for f can be reached monotonically by increasing N . Next, we substitute the approximation into the original operator equation and use linearity:

The last step involves “taking moments or weighting” both sides of the above expression.

$$L \sum_{n=1}^N a_n f_n = g \tag{3-12}$$

$$\sum_{n=1}^N a_n Lf_n = g$$

This is the same thing as saying that we take an inner product of both sides of the equation. If the inner product has been defined as

$$\langle a, b \rangle = \int_S a \cdot b \, dt \tag{3-13}$$

Where a and b are some functions of t and S is the region of validity of the functions a and b , then taking moments results in

$$\sum_{n=1}^N a_n \langle Lf_n, w_m \rangle = \langle g, w_m \rangle \tag{3-14}$$

Here we have weighted both sides of the equation with a weighting or test function w_m . The choice of the weighting function is somewhat arbitrary. If however, we choose the weighting function as being the same as the basis function. The MoM specialisation is termed *Galerkin's* method.

$$\sum_{n=1}^N a_n \langle Lf_n, f_m \rangle = \langle g, f_m \rangle \tag{3-15}$$

This effectively eliminates the difficulty of choosing a suitable weighting function and simplifies matters by making the weighting function identical to the basis function. On the other hand, the implied integration may be difficult. In this case it is sometimes expedient to choose the weighting function to be the delta function. In this case, the integration is vastly simplified and the integral equation is essentially

satisfied at a number of points. This particular choice of weighting function is therefore known as *point matching*.

Equation 3-15 represents (when expanded) one single linear equations with N different unknowns. However, it is insufficient to solve this equation unless N linearly independent equations are given. If we apply the above equation m times and expand the equation we note that we have a particularly convenient form for numerical processing. Our original operator equation has now been converted into a matrix equation with each entry of the matrix representing the operator consisting of an inner product. The unknown a_n coefficients now form the vector which can be determined by matrix inversion.

Basis functions are of fundamental importance in the computation of the unknown variables using the *Galerkin* form of MoM. There are many possible choices of basis function, however, recall that basis functions should adequately represent the current distribution. If basis functions are to be defined over the whole wire (global or entire basis functions), then the functions should vanish at the ends. Generally, the functions that best represent the unknown to be approximated are the “best choice”. On the other hand, if the wire is broken up into small sections and the current only exists over a small subinterval of the wire (subdomain basis functions), then there are less restrictions on the functions available used to represent the current. Generally, the choice of basis function comes down to a few choices with a view to:

1. Simplify the integration in the inner products.
2. Size of matrix to be handled.
3. Rate of convergence.
4. Stability of the matrix (low condition number is essential)

Most common of the two types of basis functions previously mentioned is the subdomain function. The function is a non-zero value over a portion of the $f(x')$ function domain, where the domain of $f(x')$ represents the surface of the antenna or scatterer. Subdomain functions may be used in the analysis regardless of any prior knowledge as to the characteristics of the function they are to represent. This process is particularly useful in the analysis of geometrically arbitrary orientated wires,

whereby the wire is represented by N non-overlapping segments. The most simple and least accurate of the subdomain functions used in the segmentation approach to approximate the current is the pulse function. However, there are many other functions available to represent the current distribution. Segmentation for a simple dipole illustrating its equivalent current on the surface (a) and along the centre (b) is shown below in Figure 3.6.

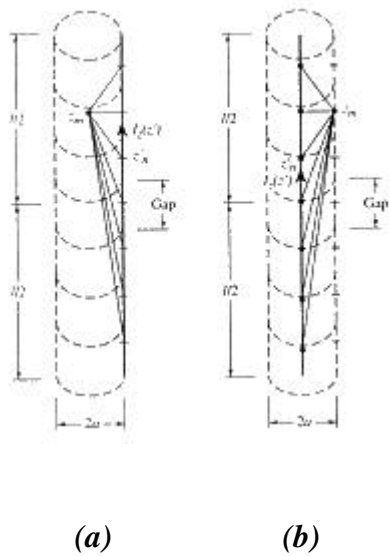


Figure 3.6. Wire segmentation of dipole showing the equivalent current (a) on the surface and; (b) along the centre [3].

The other type of basis functions: Entire domain functions are non-zero over the whole of its domain. Entire domain functions are particularly useful in applications where it is known that current distributions are primarily sinusoidal. These basis functions require fewer terms in the expansion of the matrix equations and thus require less computation time.

This concludes a review of the numerical methods used in this thesis.

Chapter 4

Computer Analysis Design

This chapter is structured from a design perspective. The various antenna simulations and design of the two different antennas (termed the indoor antenna and the mobile antenna) are discussed in detail. An iterative approach is taken with each antenna structure, whereby a basic design is first developed according to theoretical guidelines and is subsequently refined until all (or the majority of) the specifications are satisfied. This chapter will firstly discuss the design software selected for analysis followed by development of the two antenna structures. Finally, the prevailing antenna designs will be presented for fabrication.

4.1 Antenna Design Software

The antenna design software was selected for this thesis in order to allow a reasonably accurate simulation of various wire antennas. Probably the most widely accepted and one of few software packages freely available to simulate wire antennas is NEC (Numerical Electromagnetic Code). NEC was originally developed in the seventies by Burke and Poggio [9] and has since become available in a variety of formats. NEC uses a method of moments formulation with numerical integration techniques as discussed in chapter 2 to calculate current and field intensities around arbitrary wire elements. Another version of the same software package has been developed by SAIC called *EAM:NEC Fine Grain Analysis Module*, which is a windows based graphical interface for visualisation of input and output files. EAM:NEC is an acronym for Electromagnetic Antenna Modeling system for NEC. This refined version also allows faster generation of NEC input geometry files, a particularly useful attribute to this thesis since much parameter optimisation work is adopted for both antenna structures.

Although *EAM:NEC* has a superior visualisation format compared to NEC, it does however have significant limitations in graphing options for various parameters. Impedance plots on either Smith charts or linear graphs versus frequency are non-existent and have to be procured from other sources. A temporary solution to this problem has been accomplished through the use of MATLAB to read output ASCII files generated from *EAM:NEC* and to then extract the impedance and frequency information and subsequently save it into text documents. *Smith Chart for Windows* [13] is then used to read the text file and produce impedance/admittance plots.

In order to achieve reasonably accurate results in NEC, it is critical to make correct choices of segment lengths in the analyses. For this reason it is important to establish some structure modeling guidelines for NEC to maximize the accuracy of the results whilst simultaneously avoiding procedures that unnecessarily increase the computation time. Some of the more important guidelines are provided below:

- Segment length Δ should be less than about 0.1λ at the desired frequency.
- Extremely short segment lengths of about $10^{-3}\lambda$ should be avoided.
- For the standard thin-wire kernel, which assumes axial currents on segments: The ratio of segment length to wire radius should be $\Delta/a > 8$ for errors less than 1%.
- Wires should be several radii apart.

To illustrate the accuracy of *EAM:NEC*, a simple half wavelength dipole analysis is performed and then compared to theoretical results. The graph shown in figure 4.1 illustrates the accuracy of estimating the input impedance of the dipole.

The graph indicates an admittance of $7.5-j8.5$ mMho for the dipole at centre frequency, which corresponds to an impedance of $66.15 + j58.36$ Ohms. Comparing this value to the theoretical impedance of $73 + j42.5$ Ohms, it is observed that the calculated real part of the impedance provides a better approximation. The discrepancy is attributed to the finite size radius and feed model sensitivity. Provided sufficient care is taken, the simulation approaches the theoretical result. The discrepancy is not considered significant for the antennas used in this thesis.

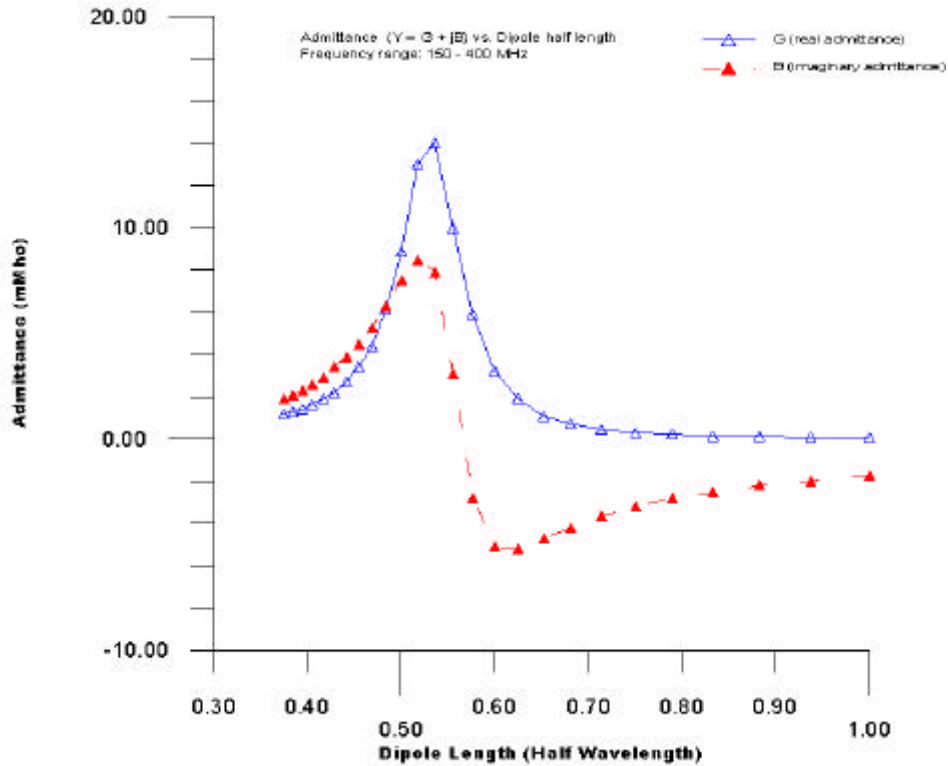


Figure 4.1 Dipole antenna behaviour (as simulated by EAM:NEC) with $L=1.0m$ and $a=0.0016m$.

4.2 Indoor Antenna Simulation

As discussed earlier the general antenna to be used for obtaining the desired electromagnetic characteristics for the indoor antenna will be a modified version of the Yagi-Uda antenna.

A summary of the technical specifications (as stated in chapter One) of the indoor antenna are repeated here for convenience:

1. Frequency bandwidth is 526-582 MHz, with centre frequency at 554MHz.
2. The input impedance is 50Ω
3. Return loss should be better than 10dB.

4. Gain should be around the 10dBi mark. Although both gain and directivity should be as high as possible.
5. Horizontal linear polarisation is required.

Three different design iterations were carried out on the indoor antenna to investigate variation of different sets of geometrical parameters and to ascertain the effects on the gain, directivity and input impedance. The experimental transition (for both the indoor and mobile antenna designs) from the first design to the third design iteration was performed with an intuitive parameter optimisation analysis. This meant varying the sensitive parameters first, working to the least sensitive parameters. This approach allows more thorough understanding of all the different geometrical parameters and their effects on the design criteria. In addition, a general trend of improvement of design specifications is observed in the design iteration process.

The geometrical parameters that significantly affect directivity, gain, input impedance etc. are of critical importance and need to be studied further. What follows is a descriptive list of the geometrical parameters that have been duly considered in the procurement of this design. The most sensitive of these parameters is analysed further in graph form.

List of variable parameters:

Number of directors (N): The number of director elements generally determines the amount of forward gain. Due to current dissipation as distance from the driven element increases, the number of directors does not significantly affect the bandwidth.

Director spacings (S_D): The element spacings all determine the coupling between the various directors. Obviously as the distance between elements is increased the coupling will decrease. Given the decrease in current as the number of directors is increased, the relationship for optimum spacings is complicated. For optimisation purposes it is possible to have unequal director spacing.

Reflector spacing (S_R): The reflector spacing changes the coupling behaviour of the other elements in the design. S_R also has an affect on bandwidth and gain.

Director length (L_D): This parameter only optimises the bandwidth criterion. The ratio of element lengths to director-to-driver length is altered to obtain the correct bandwidth.

Reflector length (L_R): The length of the reflector element affects the gain level of the back lobes of the antenna. It does however also have an effect on bandwidth. In general terms, this length is generally longer than the driver length (L) to increase forward directivity.

Driver length (L): This element is essentially a dipole element and is of critical importance for the resonant frequency of operation. Reducing the length of this element increases the resonant frequency of the antenna.

Wire radius (a): In normal operation, EAM:NEC allows only small radius wire to be used for analysis. Since the skin depth is comparatively small at the frequency of operation, there is no need to adopt a larger wire radius. In effect, changing the wire radius causes an impingement on the element spacings.

Thus, it is found that all geometrical parameters are inter-related and that each individual parameter does not have its own characteristic influence on some output variable. This is one of the fundamental reasons why designing Yagi antennas is not a particularly easy task.

4.2.1 Design Iteration One (yagi_d1.nec)

The initial design attempt of the indoor antenna features a Yagi-Uda array with a total of 6 linear wire elements: 4 directors, 1 reflector and a driven element. (The antenna geometries as well as radiation patterns and current distributions for the first two design iterations are shown in appendix C, Figure C-1 and Figure C-2 respectively).

By now examining the impedance bandwidth (as figure 4.2 illustrates), most frequency data points are within the matching circle ($VSWR = 2.0$) corresponding to a return loss of **9.7dB**. It was chosen in the specification that an acceptable return loss

for the band is 10dB. It is calculated that the pass band for the antenna exists for **527-575MHz** or **85.7%** of the total required bandwidth.

However, other important parameter requirements for the modified Yagi are the directivity and gain. The E-field radiation pattern for both elevation and azimuth at the centre frequency are for the principal plane cuts. These two cuts give a clear representation of the radiation pattern of the antenna (figure C-1). Also in figure C-1, current distributions (which also display antenna configurations) for the first indoor antenna simulation can be found along with the other design iterations. The desired radiation pattern characteristics are a noticeable front-to-back ratio, narrow beamwidth (or high directivity) and a strong attenuation of cross polarisation. It is observed that by examining the elevation pattern that the main beam is directed in the horizontal plane ($\theta = 90^\circ$) as expected. The half power beamwidth observed on the simulated radiation pattern, $\Theta_a = 41^\circ$ in azimuth and $\Theta_e = 58^\circ$ in elevation.

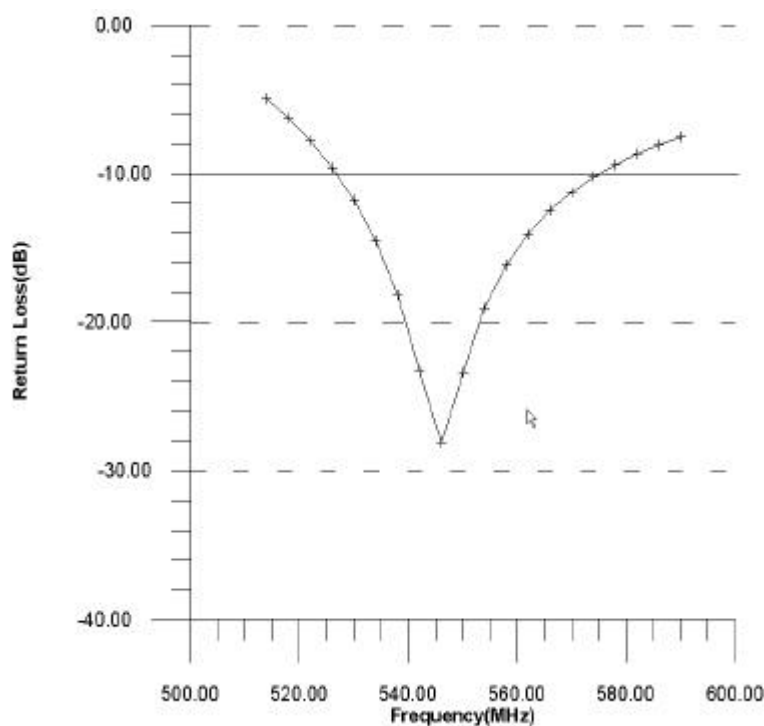


Figure 4.2. Return loss vs. frequency (generated by Grapher, ver. 1.25) for yagi_d1.out.

4.2.2 Design Iteration Two (yagi_d2.nec)

By now providing additional directors, forward gain can be significantly improved with little change to the impedance bandwidth. It will also be noticed that additional reflector elements have been included as part of the main structure for design two. This ‘wire grid structure’ provides a more effective reflector for the antenna over and above a simple single wire reflector. It also serves to increase the power gain of the antenna in the forward direction (Figure C-2), thus increasing the front-to-back ratio.

The impedance bandwidth for the design is given below in Figure 4.3. Compared to design number one, it is observed that the bandwidth is now **91.1%** of the total bandwidth, i.e. passband exists for **527-578MHz**. By also comparing the E field radiation patterns for yagi_d1.nec and yagi_d2.nec (Figures C-1 and C-2), it is observed that a slightly more acceptable beamwidth is now obtained, i.e. $\Theta_a = 38^\circ$ and $\Theta_e = 55^\circ$.

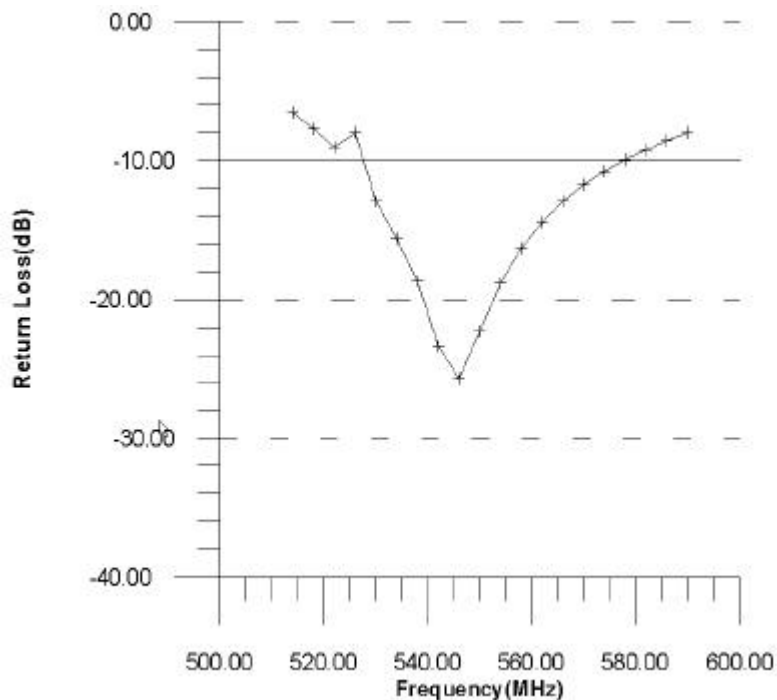


Figure 4.3. Return loss vs. frequency for yagi_d2.out.

4.2.3 Design Iteration Three (yagi_d3.nec)

In design number two, a number of closely spaced reflectors has been used together to produce a higher forward gain of the antenna. By extending the distance between the reflector elements, a larger effective reflector is created resulting in a larger surface over which the incident wave is reflected.

The next step in the design procedure is to decrease the angle of the reflector plane in an attempt to further increase the gain without affecting the bandwidth. In effect, the reflector plane created in the previous paragraph is a fundamental corner reflector with an angle of 180 degrees. Results have proved that reduction of this angle increases the gain in the forward direction. The first obvious choice is to change the angle to 90 degrees and observe the effects. Impedance bandwidth is significantly reduced mostly due to the differing distances between the various points on the reflector elements and the driver. Adjustment of S_R is needed to improve the bandwidth. An optimal S_R value of **0.228m** was found, which is far too large for the indoor antenna specification was not considered further.

By now decreasing the angle of the reflector plane to an angle of 135 degrees, the bandwidth is less affected by the angle change and considerably smaller adjustments to the driver reflector distance can be made to correct the bandwidth. This option has introduced only slight reduction in gain.

Another option worthy of investigation is the possibility of using a circular parabolic reflector. According to theory [5] more directivity can be obtained given a physical size of antenna with a parabolic reflector for aperture plane greater than 2 wavelengths. However, the effective aperture of design number three is less than one wavelength, hence it would be more worthwhile adopting corner-type reflectors for gain improvement. In addition, we must keep in mind that, the size of the antenna must be kept to a minimum.

The simulations have proven that using square mesh, a power gain of **9.3 dB** is obtained using angled reflectors with a subtended angle of 135° with slight adjustment

to spacing between driver and grid-mesh to compensate for any bandwidth deficiency. Figure 4.4 shows that beamwidths of $\Theta_a= 35^\circ$, $\Theta_e= 52^\circ$ were achieved using the geometry in yagi_d3.nec. Adopting a parabolic reflector it was found that the gain is only **0.1 dB less**, but the **bandwidth is seriously degraded**. The current distribution, which incidentally indicates the general geometry for yagi_d3.nec is shown below in Figure 4.5.

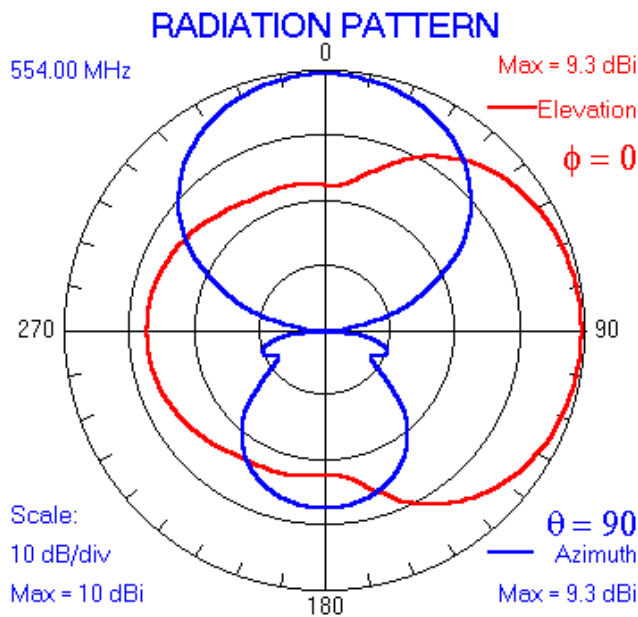


Figure 4.4 Radiation patterns for final Indoor antenna prototype

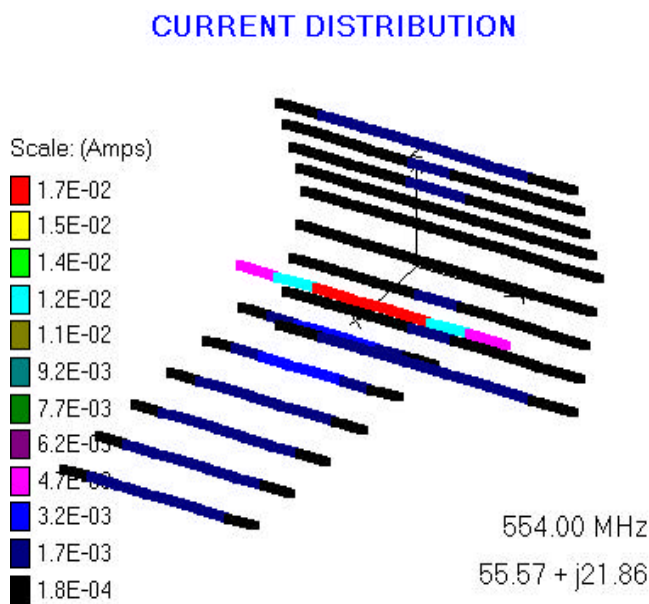


Figure 4.5. Current distribution for yagi_d3.nec

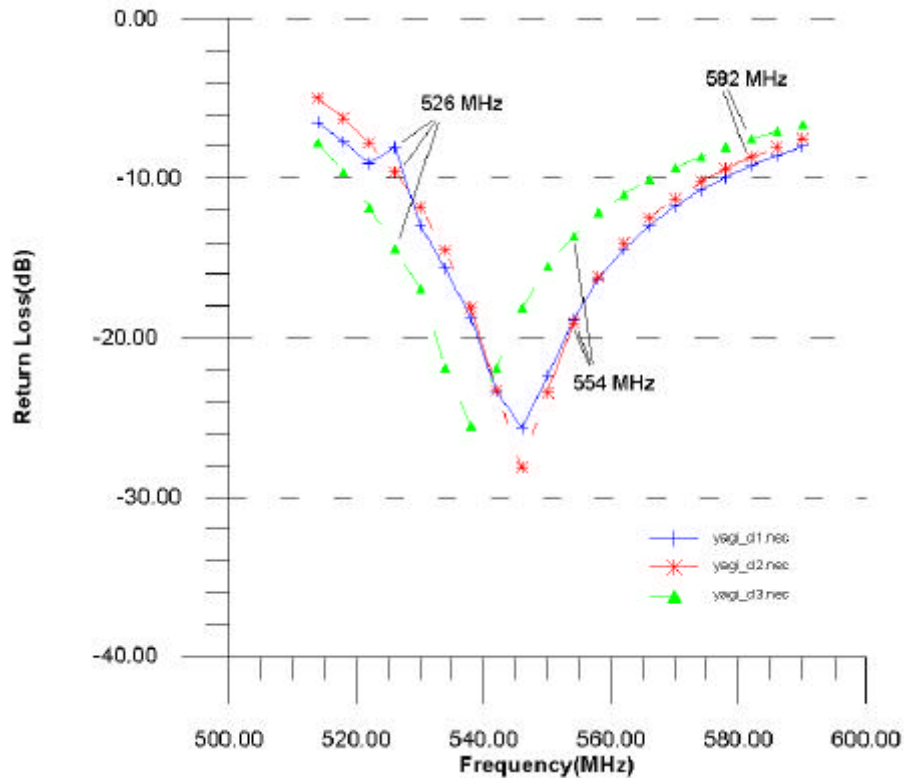


Figure 4.6. Impedance plot of all three modified Yagi-Uda designs.

Figure 4.6 shows that the bandwidth of yagi_d3.nec compared to that of yagi_d2.nec and yagi_d1.nec is slightly less than desired, with the passband existing from **518-575MHz** or **87.5%** of the required bandwidth. Although, the bandwidth is somewhat less than anticipated, it is envisaged that some adjustment of the final Indoor antenna prototype: yagi_d3.nec may be needed in the feed area to get the correct resonant frequency.

4.3 Design of Feed network for Modified Yagi

Design of inaccurate feed networks between feed line and antenna can result in high VSWR or undesired radiation patterns leading to high power losses in the system. For example, direct use of a coaxial line applied to the feed point may result in the radiation pattern perturbation. By employing a ‘balun’ (term coined from balanced-unbalanced), the RF signal is prevented from returning down the outside of the coax

feedline and subsequently providing additional power losses and uncontrolled radiation.

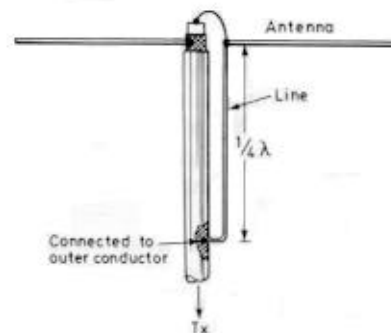


Figure 4.7. The bazooka balun [14]

Judd [14] suggests that the most suitable balun for a dipole element is a ‘bazooka’ balun. The driven element on the modified Yagi design is very similar to a dipole, but slightly shorter in length. The diagram in Figure 4.7 above illustrates the construction of the bazooka balun. Notice the use of the quarter-wave line section soldered to the one end of the dipole and the other end to the outer of the coax line. This line may be slightly altered because of the fact that the antenna in question is being matched to 50Ω rather than 75Ω .

4.4 Indoor antenna – Mechanical Design

The mechanical design and construction of any antenna plays a crucial role in the antenna design procedure. Both antennas discussed in this thesis must be mechanically designed in such a way that the antenna will be able to support itself and still not significantly interfere with the electrical parameters of the design. With these thoughts in mind, mechanical design attempts are discussed for both antennas.

The wire selected is brass tubing, which is quite suitable for wire antennas for some important reasons. It is self-supporting, ie. it has a low tendency to flex or bend at

long lengths and is lighter in mass as compared to solid tubing. It has a relatively high conductivity, $\sigma = 2.56 \times 10^7$ and low small skin depth compared to other materials at the frequency of operation. By using simple electromagnetic theory it is calculated that the skin depth of brass at the centre frequency of 554MHz is 4.337 μ m. The thickness of the wire wall used in the design is approximately 0.3mm, resulting in 69.17 skin depths, which is well sufficient.

The material for the support booms is selected such that a relatively high dielectric constant is exhibited and consequently a small likelihood of scattering the electromagnetic radiation. Wood is generally discarded due to its porous nature and ability to conduct when moist. For this reason, grey PVC with a dielectric constant of around 4.0 is chosen for the support structure.

Referring to the schematic diagram in appendix A.1, the position allocated for the dielectric spacers have been carefully chosen so as to have the least impact on electrical radiation characteristics. By examining the current intensity over the pass band, locations of minimal current density have been located and recorded on the schematic. In general, the spacers are kept out of range from particularly sensitive area such as the driven element. The spacers are constructed of the same material as the plastic support beams.

Construction of the base support structure is situated around the phase centre of the antenna (in this case the driven element or feed network). Some amplitude and phase errors are expected to be prominent when the radiation pattern of the antenna is measured on the test range. However, only a minute amount of this error is expected to be due to the position of the antenna phase centre at such a low frequency of operation.

4.5 Mobile Antenna Simulation

It was initially envisaged, at the beginning of this thesis, that an array modified folded dipole antennas be used to construct a mobile receiver.

Many of the design specifications of the DTV antenna for use with mobile receiving purposes are the same as for the indoor antenna. The most obvious difference however, being the requirement for an omni-directional azimuth radiation pattern.

Below is a summary of the required specifications for the mobile DTV antenna:

1. Frequency bandwidth is 526-582 MHz, with centre frequency at 554MHz.
2. The input impedance is 50Ω
3. Return not loss less than 10dB.
4. Gain should be as high as possible
5. A horizontal polarization is required.
6. An omni-directional azimuth pattern

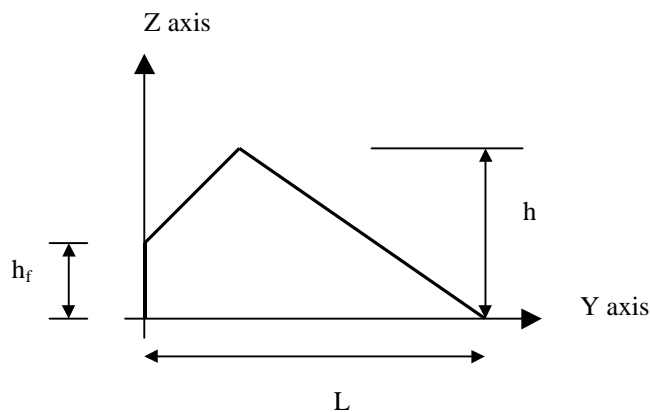


Figure 4.8. General configuration for mobile antenna

All of the antenna designs for the mobile receiver utilise inclusion of a ground plane. Since these designs are theoretically envisaged to be used in a vehicular application (i.e cars, trains, etc.), where a ground plane is readily available. Figure 4.8 describes the general geometry adopted for the mobile antenna describing all of the parameters used in the design.

4.5.1 Design Iteration One (h_rhomb.nec)

The design method for obtaining the requirements for the mobile antenna design will be such that the radiation patterns will be optimised first, and the impedance bandwidth optimised secondly. This warrants the extremely poor bandwidth obtained in h_rhomb.nec. The gain of the half rhombic loop is similar for both radiation patterns, at ~ 5.5dBi. Like the indoor antenna designs, Figure C-3 and C-4 in appendix C.2 contain all the radiation patterns and current distributions for the first two mobile antenna design iterations.

4.5.2 Design Iteration Two (spider1.nec) - Wideband design

The design particulars of spider1.nec extends the half rhombic loop reflected in the ground plane into **four directions** to increase the gain and distribute the directivity of the azimuthal pattern more evenly. Several adjustments to other parameters were required to obtain a more correct bandwidth. In particular, the height of the feed above the ground plane proved to be a particular sensitive geometrical parameter for bandwidth adjustment.

Due to the acuteness of response to alteration of the feed pin height, h_f , a sensitivity analysis was conducted in order to obtain the most suitable value for optimum bandwidth. Below is a graph comparing the effects on bandwidth of varying the height of the feed above the ground plane.

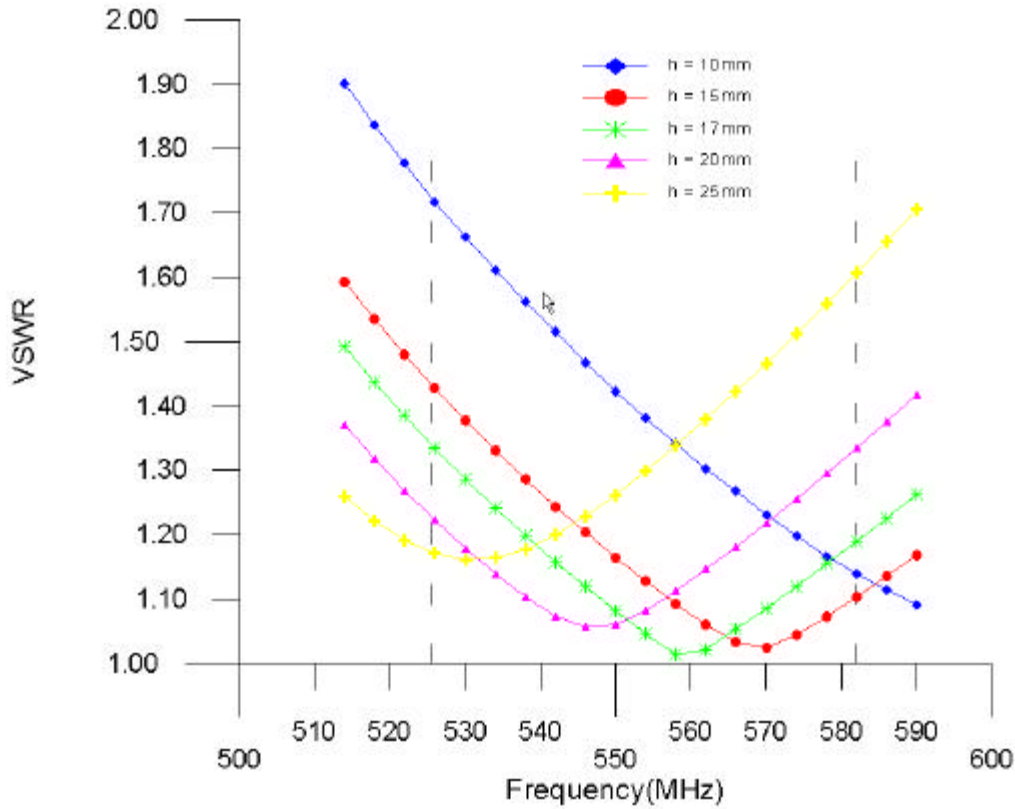


Figure 4.9. h_f parameter sensitivity analysis

The final percentage bandwidth of spider2.nec obtained was **490-655MHz** or **30%**, indicating a **wideband** design. Although the impedance bandwidth criterion is easily satisfied, it would be more appropriate to obtain an impedance bandwidth more suitable to the required bandwidth, 526-582MHz. In addition, the radiation patterns obtained for spider2.nec show a noticeable fluctuation in the directivity as a function of θ of the azimuth pattern. This is not quite correct for omni-directional standards, and needs to be distributed more evenly. The gain at centre frequency obtained for the elevation and azimuth patterns are **6.1dBi** and **5.8dBi** respectively. It would be considered, at this stage, that the gain obtained for spider2.nec is sufficient for this thesis.

4.5.3 Design Iteration Three (spider2.nec)

To improve the characteristics of design iteration two, we see that the bandwidth needs to be reduced quite considerably. Also, as mentioned previously, we see that the omni-directional radiation pattern is **1dB less** at $\phi = 45, 135, 225$ and 315 degrees. With regard to the second requirement, it was found that by reducing the number of legs on the spider to **three**, a greater uniformity in the directivity is obtained. By examination of the elevation radiation pattern shown below, it is seen that the beamwidth, is slightly increased (an undesirable characteristic which leads to smaller attenuation of vertical signal components), compared to the elevation pattern for spider1.nec. However, inquiry into the azimuthal pattern shows a more omni-directional characteristic with smaller directivity fluctuations, compared to spider1.nec.

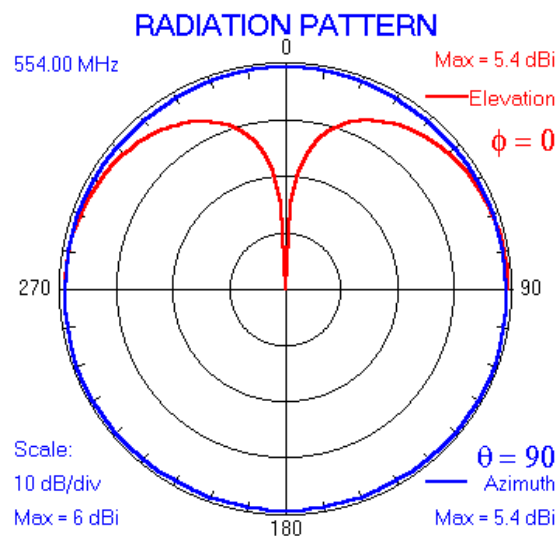


Figure 4.10 Radiation patterns for final Indoor antenna prototype

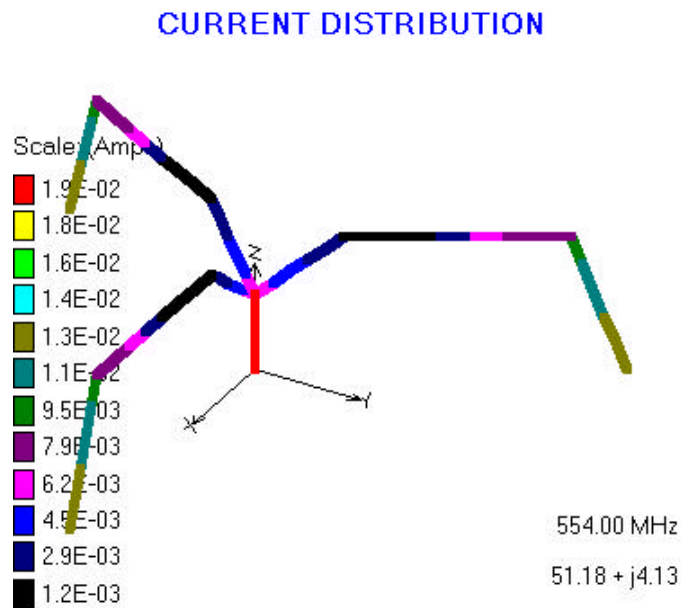


Figure 4.11. Current distribution for spider2.nec

Ideally a more sensitive scale on the radiation pattern plots would show greater detail of any E-field fluctuations. Unfortunately however, EAM:NEC does not have this capability thus compromising an investigation into a more detailed analysis.

The gain of spider2.nec is somewhat reduced in elevation: **5.4dBi** and azimuth: **5.2 dBi** compared to previous designs. However, the impedance bandwidth criterion takes precedence over the gain of the antenna.

Then by re-adjusting the height of the feed above the ground plane up to 40mm, the bandwidth was reduced to the specifications, i.e. **526–582MHz** corresponding to 100% of the required bandwidth. By also examining the return loss graph in Figure 4.12, it can be seen that the minimum return loss is **11.725dB** or a VSWR of **1.80**, which is quite acceptable.

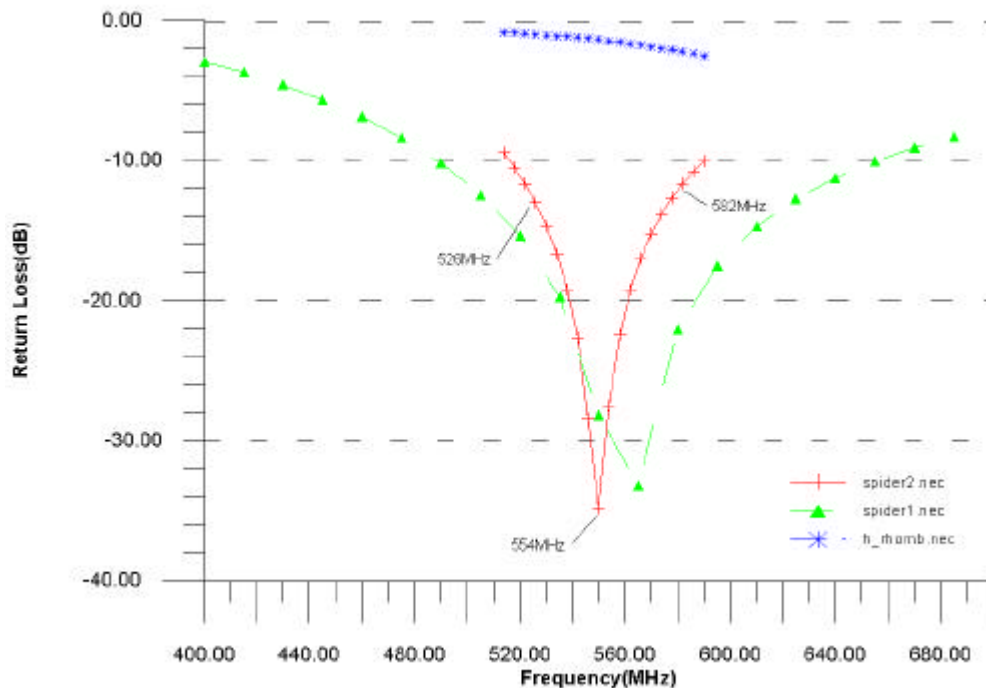


Figure 4.12. Comparison of the return loss for all three Mobile antenna design iterations

4.6 Mobile antenna – Mechanical Design

The last design iteration of the mobile antenna: spider2.nec is easier to mechanically implement compared to the modified Yagi-Uda antenna. The use of a ground plane increases the rigidity of the antenna, thus avoiding the requirement of additional dielectric support material, thus avoiding any partial obstruction that could modify the electromagnetic coupling behaviour.

Implementation of the feed network however, has posed a somewhat more formidable challenge. Using a SMA bulkhead connector connected to the underside of the ground plane serves as the connection point. Due to the high sensitivity of percentage bandwidth on the height of the feed above the ground plane (as pointed out earlier), an extended section of machined teflon dielectric sheath is placed over an extension wire to provide a support ledge on which the “spider-legs” sit. Appendix A.2 shows the full schematic.

4.7 Dipole Transmitter antenna – Mechanical Design

The frequency band of operation, 526-582 MHz is far too low in the frequency spectrum to make use of a standard transmitter antenna, which are unavailable at the above band. To combat this, a dipole transmitter must be designed and fabricated in order to transmit the RF signal with minimal power losses.

For radiation pattern measurement purposes it is required to have all of the directivity in a forward direction. By implementing a ground plane spaced at $\lambda/4$ below the dipole this can be achieved. The dipole antenna transmitter is matched at $Z_o = 50\Omega$, by purposely designing the length of the dipole longer than $\lambda/2$ and then trimming the antenna back with pliers to get the required impedance. Below is a sketch of the dipole transmitter antenna including dimensions. A photograph describing the mechanical detail of the transmit antenna is shown at the end of appendix A.3. Further discussion of the S_{11} /return loss measurements for the transmitter antenna will be presented in the next chapter.

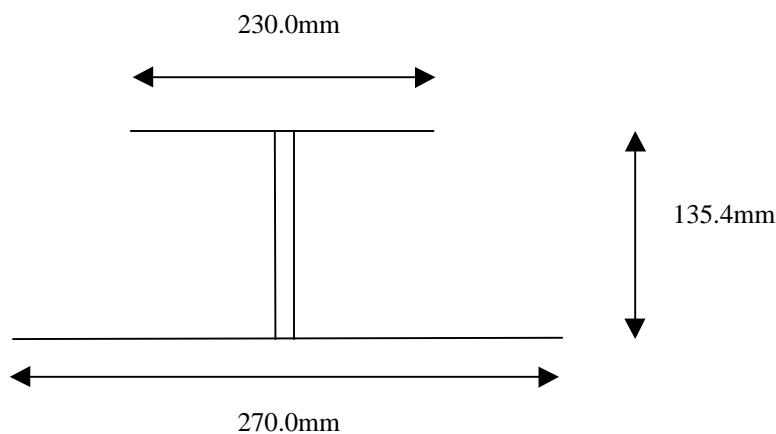


Figure 4.13 Dipole transmit antenna side view configuration.

4.8 Sources of possible error

As we noticed earlier with the impedance analysis of the dipole, it was discovered that some discrepancy with impedance matching. We can already expect that the results will be somewhat in error due to the computational limits in *EAM:NEC*.

There are also several other different sources of potential error in addition to the *EAM:NEC* limitation. A few of the more significant error sources will now be discussed.

The far-field test range is designed for frequencies of 5GHz and upward with the absorber material also designed for the same frequency range. This will produce a certain amount of reflection from the walls and will hence produce phase and amplitude errors in the radiation pattern/gain measurements.

Another phenomenon worthy of particular mention is the addition of dielectric material to the antenna structures (particularly the Yagi-Uda). Dielectric material added to conducting wire has the characteristic effect of increasing the electrical length of the conductor. *EAM:NEC* does not model this dielectric material and so some disagreement with experiments is expected here.

It is also expected that the feed on the Yagi will be particularly sensitive and some trial-and-error adjustment work may be needed to obtain a good impedance match and corresponding radiation patterns.

Chapter 5

Measurements

Chapter 5 is sub-divided into two major sections. The first section will briefly discuss particulars of the measurement equipment including status of the anechoic measurement chamber at UQ. Secondly, the results incorporating return loss, radiation pattern measurements and gain calculations of the two final prototype designs will be presented in detail, including comparisons to simulated data.

In addition to the above, some of the discrepancies between the measured and simulated design data due to inevitable error sources will be analysed as well as temporary solutions implemented to combat these erroneous effects.

5.1 Measurement Setup

Due to the relatively low frequency of operation, and high level of directivity, the modified Yagi antenna is a suitable candidate for the near-field testing facility. It is however, a different situation for the mobile DTV antenna for it features an omnidirectional azimuth radiation pattern, a typical characteristic which cannot be measured on the near-field range. For this reason, (and to avoid complications associated with learning two different measurement techniques) the far-field range connected to the Vector Network Analyzer (VNA) is chosen for radiation pattern and return loss measurements of both DTV antenna designs. The far-field criterion has been adequately satisfied at the frequency bandwidth, as shown in equation 5-1 below:

$$R \geq \frac{2D^2}{\lambda} = 0.591m \quad (5-1)$$

where D is the largest aperture dimension (Aperture plane, $D = 0.4\text{m}$)

λ is the wavelength (take $\lambda_0 = 0.5415\text{m}$)

This value of R compared to the physical distance between dipole transmitter (approximately 3.25 metres) ensures that far-fields are measured. The anechoic chamber situated at UQ is presently designed for frequencies greater than 5GHz. This is a problem for low frequency measurements, as the absorber material will reflect somewhat the incident electromagnetic fields. One possibility to improve the radiation characteristic of the dipole is the use of **Time Gating Methods**, although these are usually reserved for wide-band designs. A simplified block diagram of the system interconnection between the motor-controlled antenna mounting platforms, anechoic chamber and the VNA is shown below in figure 5.0.

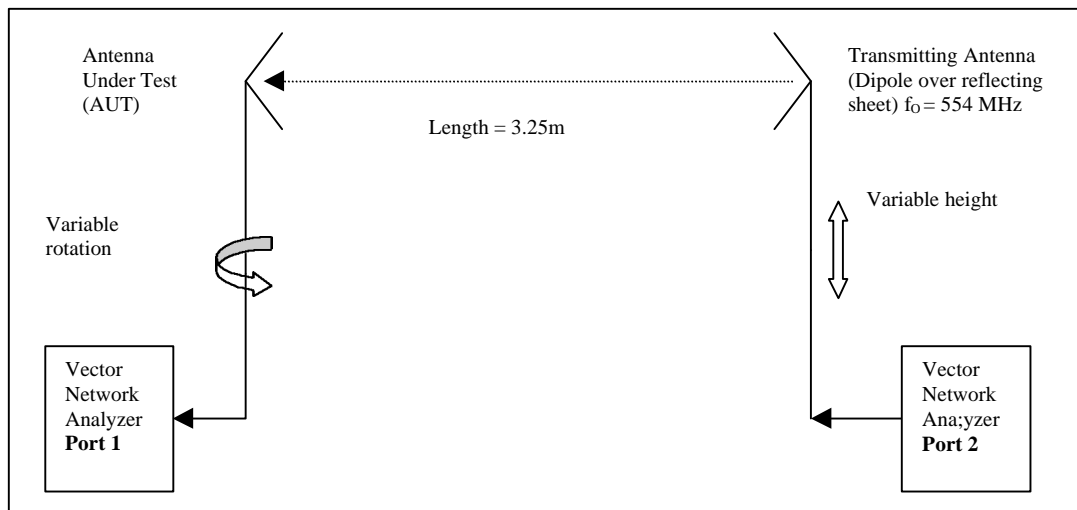


Figure 5.0 Measurement setup within the Far-field anechoic testing facility

5.2 Gain Calculation using Numerical Integration

The usual method for estimating gain measurements is by using the **Three-antenna method**. The method would involve construction of a third antenna in addition to the receiving antenna and transmitting antennas used in this thesis. It would nominally

also consist of a standard dipole to be used to provide a reference gain for the receiving antenna prototype, hence providing a measured gain relative to a dipole antenna. However, due to time restrictions and other factors only one transmitter dipole antenna could be implemented, thus discarding the possibility of using the three-antenna method.

Although this method could not be used, other possible methods also exist allowing estimation of the directivity and gain by means of computer programs. There are two different mainstream methods available for calculating directivity and gain [3]:

- **Option 1:** By using **Kraus's formula** (equation 5-2), which requires estimation of the radiation efficiency (e_{cd}) and approximate values for the 3dB-beamwidths (Θ_{1r} , Θ_{2r}) in the two orthogonal planes. Note that this method is only a rough estimation of the directivity and gain.

$$D_o = \frac{4p}{\Omega_A} \cong \frac{4p}{\Theta_{1r} \Theta_{2r}} \quad (5-2)$$

$$G = D_o e_{cd} \quad (5-3)$$

- **Option 2:** By constructing a computer program to numerically integrate the radiated power (or radiation pattern data from VNA), directivity can be obtained through combining equations (5-2) and (5-3) with (5-4). Where $F(\theta, \phi)$ is simply the combination of the two radiation patterns in azimuth and in elevation. We note however, that this method also requires estimation of the radiation efficiency.

$$\Omega_A = \frac{\left[\int_0^{2p} \int_0^p F(\mathbf{q}, \mathbf{f}) \sin \mathbf{q} d\mathbf{q} d\mathbf{f} \right]}{F(\mathbf{q}, \mathbf{f})|_{\max}} \quad (5-4)$$

It is considered that estimation of e_{cd} will yield inaccurate directivity calculations leading consequently to incorrect gain values for the antenna designs. For this reason, the methods described above have not been pursued further.

5.3 Dipole Transmitter Antenna

The Dipole transmitter antenna was initially discussed in chapter four. The results of the return loss measurements of this antenna will be presented here along with a discussion of implications of results

The dipole length of the antenna was trimmed to obtain a resonant frequency of 554MHz. The return loss for the dipole antenna is shown below in Figure 5.1. The plot shows that at centre frequency (actually **554.5MHz**), a good return loss of **26.51dB** is obtained. However at the band edges, a considerably worsened return loss is evident: around **6dB**. Although a return loss better than 10dB is desired over the entire band, it is anticipated that negligible effect of the return loss will occur in the radiation characteristic of the dipole antenna (which is the major purpose for construction of the dipole transmitter).

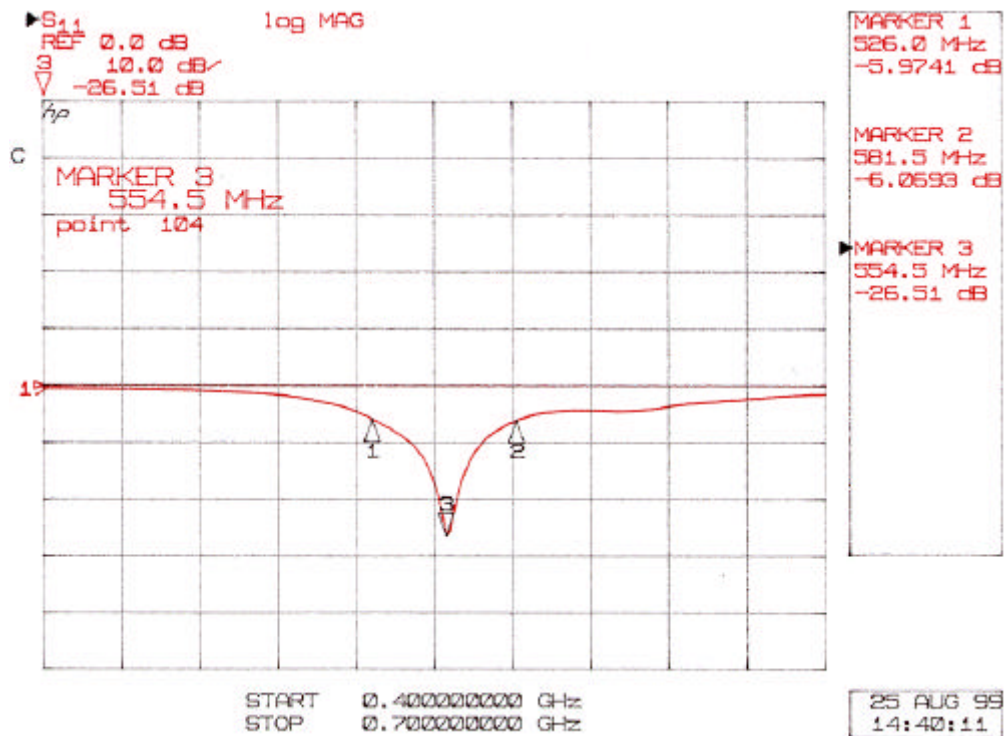


Figure 5.1. Return loss of transmitter.

5.4 Measured Results

Two different S-parameter measurements were performed on both antenna design prototypes to procure quantitative results for comparison with simulated data. S_{11} -measurements (or return loss) yielded data sufficient for estimation of the impedance bandwidth of the antenna prototypes. S_{21} -measurements (or coupling) were used to give comparisons of the radiated power and allowed consequent calculation of 3dB-beamwidths, directivity, and gain.

A comparison of the above measurements with simulated data (from EAM: NEC) have been conducted to provide indications of the validity and accuracy of the measurements. A detailed comparison of predicted and actual return loss measurements (as seen in figures 5.2 and 5.4) have been implemented by converting results formats using MATLAB computer programs. However, visual inspections of

radiation pattern data have sufficed for comparison purposes due to a more complicated nature of output format.

5.4.1 Indoor Antenna Prototype

The return loss measurement as a function of frequency of the indoor antenna prototype as generated from the VNA along with a comparison to the theoretical simulations is shown below. By initial examination of the plot, it is noted that the S_{11} data trend is similar to simulations as predicted earlier in Figure 4.6. A comparison has of theoretical and actual return loss results are shown in Figure 5.2.

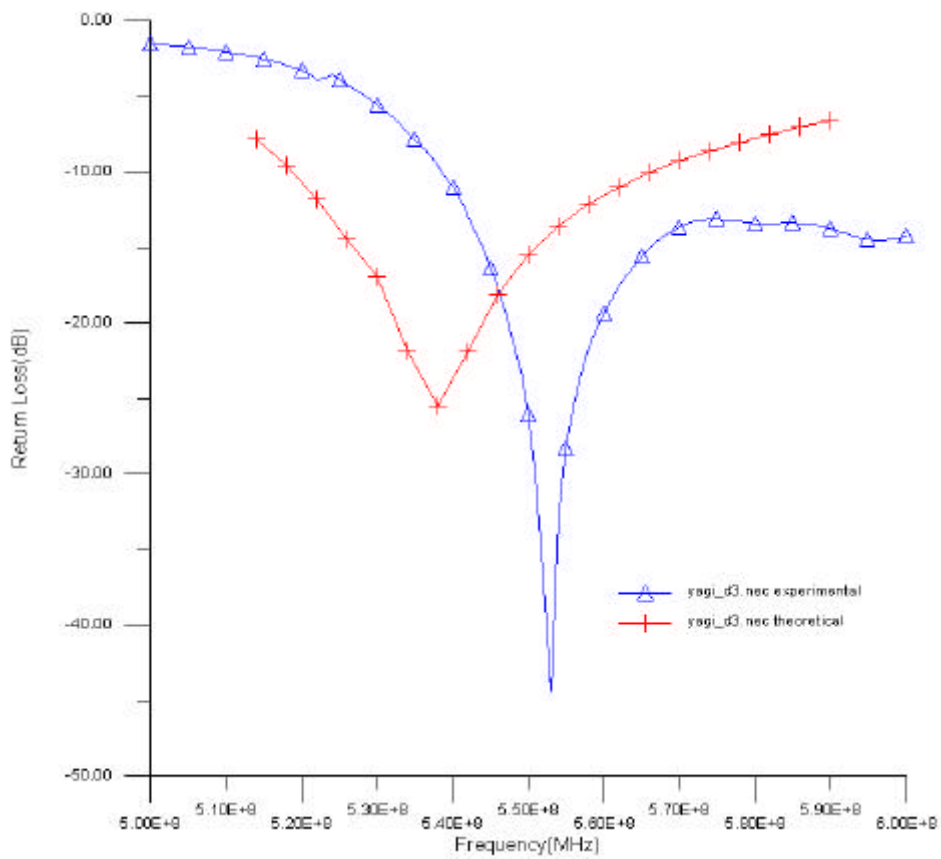


Figure 5.2. Comparison of return loss measurements to simulated data of *yagi_d3.nec*.

However, there have been some noteworthy alterations made to the feed of the indoor antenna prototype in order to arrive at the final result shown in Figure 5.2. The driven element consists of a simple dipole with a balun attached. Discussed thoroughly in chapter four, the simulated return loss behaviour of the dipole antenna was not precise at the resonant frequency. In fact, the dipole actually resonated at a length slightly greater than the theoretical resonant length of $\lambda/2$. To compensate for the decrease in return loss observed, adjustment of the voltage delta-gap and hence the overall length of the dipole to achieve the desired return loss was performed. In addition, it was also observed that attachment of the ‘bazooka’ balun (discussed in chapter four) generally produced no improvements on the return loss. By placing both of the antenna prototypes within the anechoic chamber whilst performing the S_{11} measurements, better isolation from electrical noise was attained.

Two primary axis cuts of the radiation pattern measurements were performed on the final Yagi prototype. Overall, greater accuracy in regard to comparisons with the theoretical radiation characteristics was achieved. Attachment of the balun to the feed of the antenna proved critical to obtain symmetrical radiation patterns.

The azimuth pattern was first measured by simply erecting the antenna onto the plastic-mounting cylinder (illustrated in Appendix A: Photos of antenna prototypes). The measurements obtained for the azimuth pattern of `yagi_d3.out` is shown in Figure 5.3.

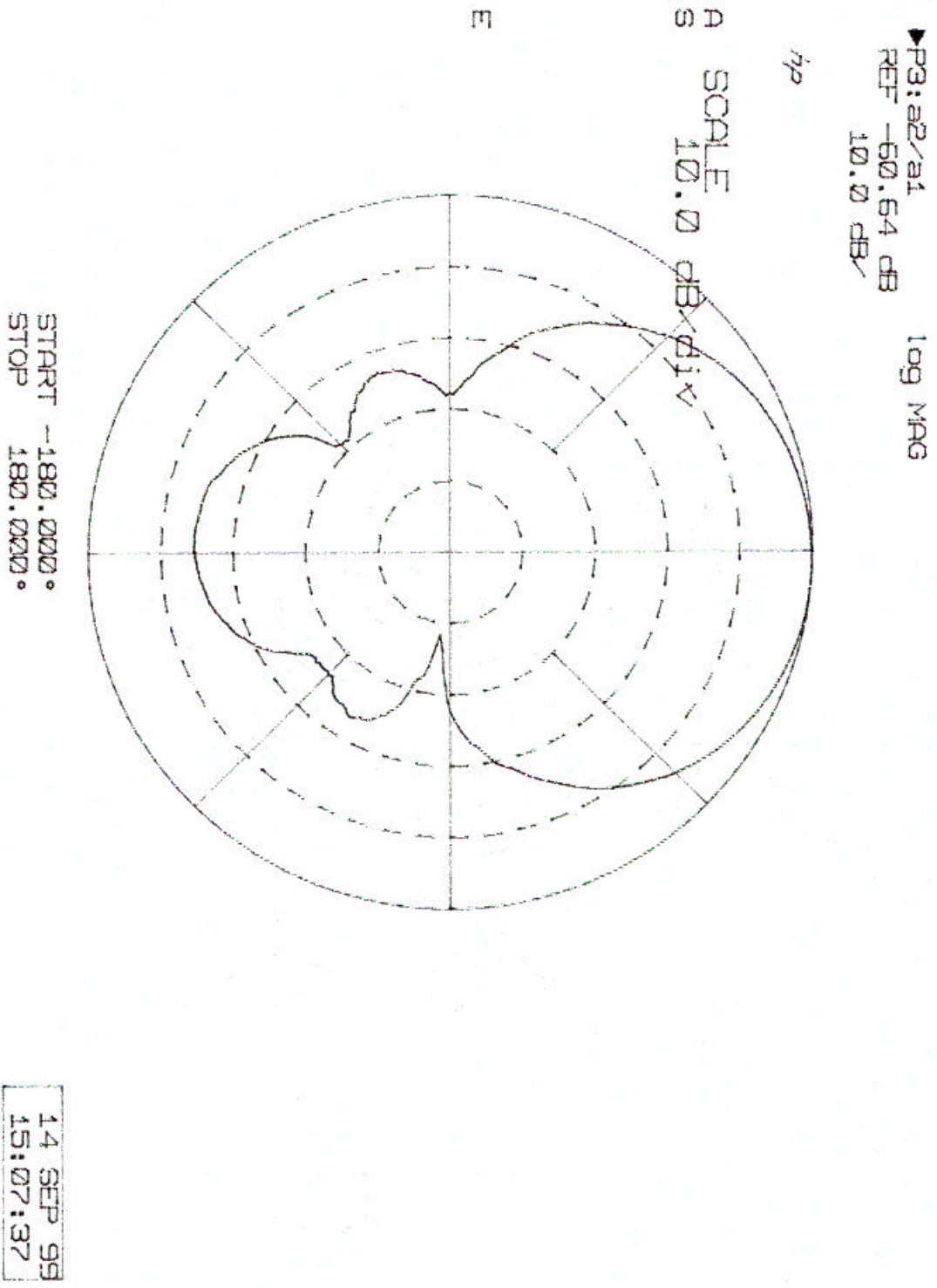


Figure 5.3. Measured azimuth radiation pattern for yagi_d3.nec

Measurement of the elevation pattern of yagi_d3 was unable to be performed due to the fact that the coaxial cable (connected to the feed at one end) was not sufficiently long enough to reach the SMA connector on the mounting plate (with the right-angle mechanical jig in place). Although a longer cable could be stripped and utilised as a second feed cable, it would not have maintained the consistency of measurements leading to incorrect directivity and gain calculations anyway. It can be appreciated, however that by viewing the pattern attained with the transmitter antenna rotated into vertical polarization shows a negligible signal levels (Figure D-1 in appendix D).

Gain calculations for the indoor prototype were unfortunately unable to be performed using the options described in section 5.2 due to insufficient data, i.e. Elevation pattern was not completed thus forming an incomplete $F(\theta, \phi)$.

5.4.2 Mobile Antenna Prototype

In general, the mobile antenna prototype measurements were performed with fewer complications than the indoor case. Comparisons of theory with experimental results for return loss measurements of the mobile antenna show many similarities. With reference to Figure 5.4 below, it is noticed that a similar shift in resonant frequency for the measurements is attained compared to the Yagi prototype. However, unlike the Yagi, both the centre frequency as well as the band edges are below the required 10dB return loss, thus meeting the required specifications.

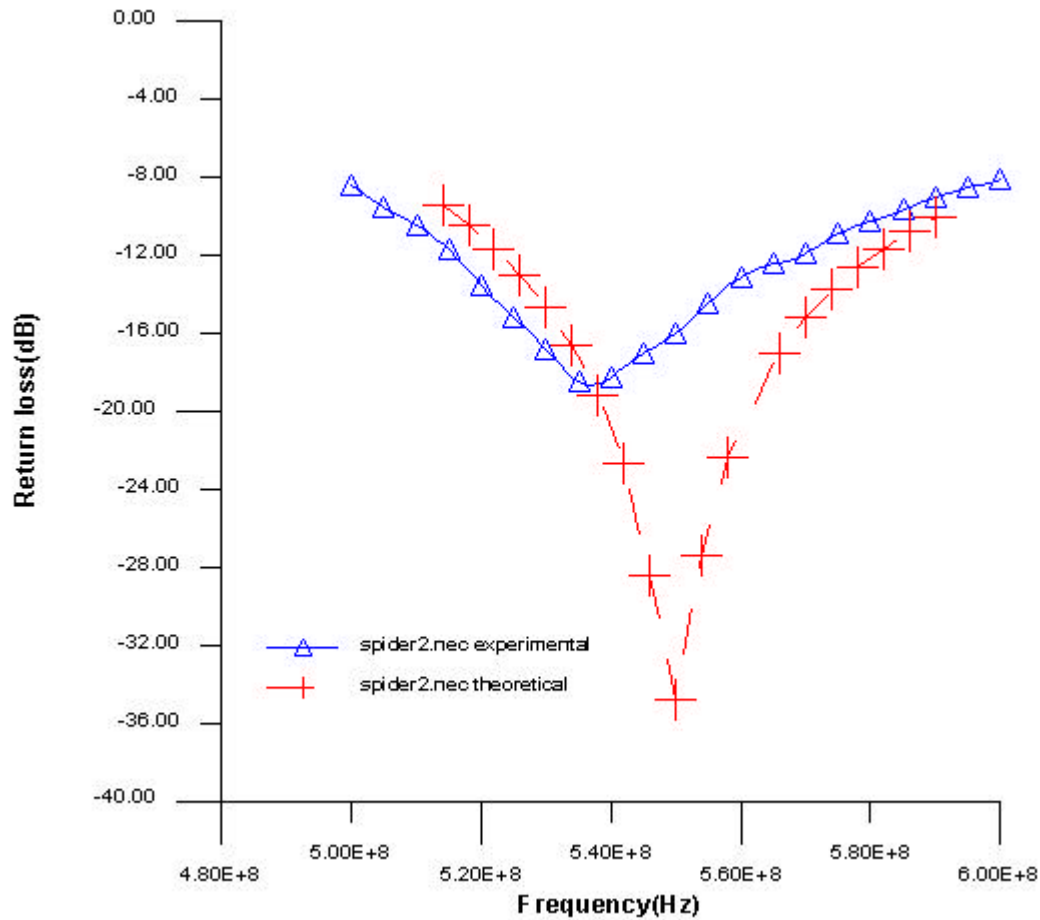


Figure 5.4. Comparison of return loss measurements to simulated data of spider2.nec.

Ideally, variation of the feed height, h_f would have produced more accurate correlation to the theoretical data. This would have produces smaller differences between amplitude of both data sets at a specified frequency. Although adjustment of the driven element was performed in the Yagi design with relative ease, it is considerably more difficult to repeat a similar procedure with the mobile design due to the mechanically fixed feed height of the antenna.

In regards to radiation patterns, it is noticed that an approximate **15dB** attenuation of signal components in the $\theta = 0$ degrees is present. Although in simulations the attneuation is far larger (more like 40dB), greater measurement accuracy is required for better correlations with the simulated radiation elevation pattern. Theory [3]

suggests that reflections from the walls produce interference patterns causing the radiated power to 'round off' (Figure 5.5 and 5.6).

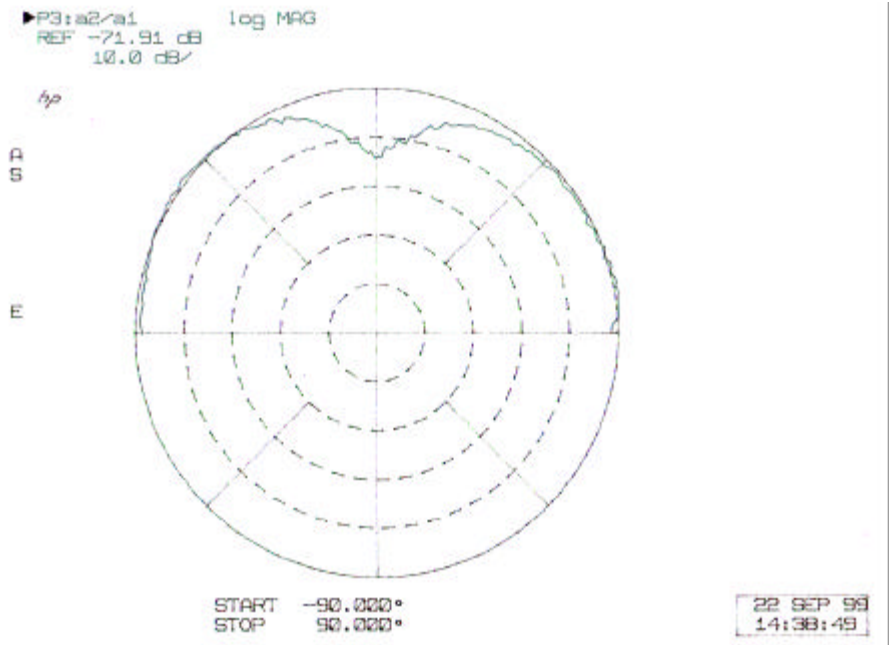


Figure 5.5. Elevation Pattern for spider2.nec (experimental)

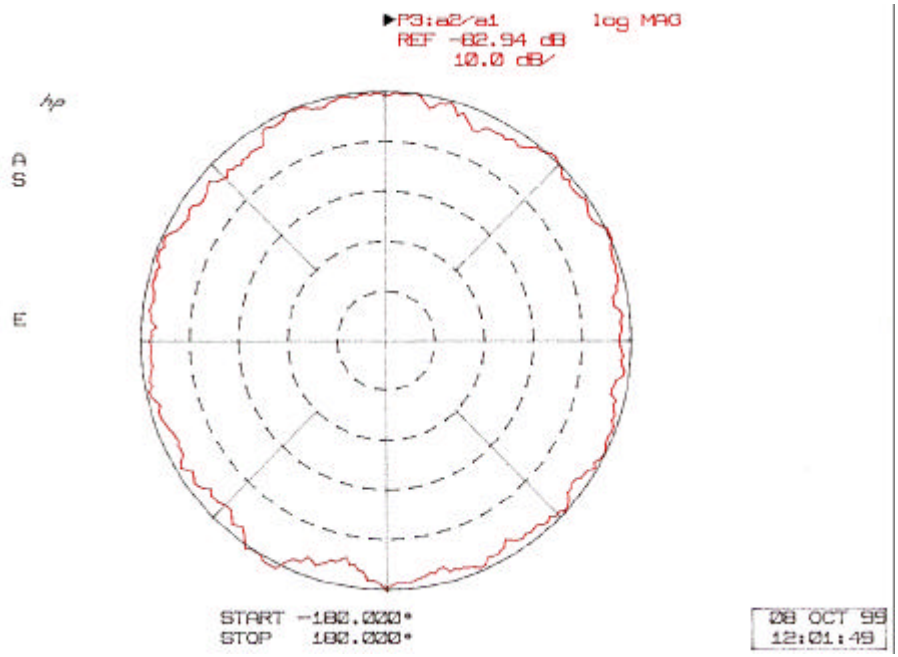


Figure 5.6. Azimuth Pattern for spider2.nec (experimental)

Chapter 6

Conclusions

In summary of the results for the both the indoor and mobile antenna prototypes discussed in Chapter 5, a table is illustrated below, which outlines the values of the major design parameters deemed important in procurement of each design.

Specifications	Indoor Prototype (after modifications)	Mobile Prototype (no modifications)	Ideal
Percentage Bandwidth	8.4%	10%	526-582MHz or ~10%
Front-to-Back Ratio	15.2dB	-	15dB
Cross polarisation	20.1dB	15.4dB	15-20dB
Minimum Return loss	45.15dB	19.78dB	26dB (Indoor) 34.5dB (Mobile)

It is noted that the indoor prototype (after modifications to the feed area) has met all but one of the requirements given in the specification. Although the impedance bandwidth, (actually 535-600 MHz) is not quite as required, it was found that the return loss parameter is sensitive to any slight adjustment in driven element length of the antenna. Similarly for the Mobile design, most of the specifications were satisfied according to table above.

It is unfortunate that the gain measurements were not possible. Although an assumption of the radiation efficiency (eg. $\epsilon_{\text{rad}} = 95\%$) of the antenna may have been reasonable for an estimate gain calculation, it would have been preferable to implement the three-antenna method for directivity and gain calculations.

The design and testing procedure could have been performed differently. By firstly implementing one of the earlier design iterations, any formidable problems with structure of the antenna may have been highlighted. Also, the design specification in chapter one could have been made more explicit to develop more up-to-date designs.

Some ideas and proposals for future work in regard to both designs are discussed below.

The yagi antenna should maybe incorporate some mechanically adjustable feed spacing device for impedance tuning in marketable versions of this antenna. It is also interesting to note that the second design iteration of the mobile antenna – spider1.nec is a possible candidate antenna for a wideband design to cover more than one of the original transmission bands.

A Similar option may be possible for the mobile antenna, although will be adjustable feed height. Mobile has better impedance match. Can say that the feed area of wire antennas not modelled very well by NEC

Bibliography

- [1] Australian Broadcasting Authority, *Australian Broadcasting Planning Handbook for Digital Terrestrial Television Broadcasting: DRAFT*, 12 November 1998.
- [2] http://www.ebu.ch/dvb_news/dvp_pr047.htm
- [3] Constantine A. Balanis, *Antenna Theory: Analysis and Design*, John Wiley & Sons Inc., New York, 1997.
- [4] Warren L. Stutzman and Gary A. Thiele, *Antenna Theory and Design*, John Wiley & Sons, New York, 1981.
- [5] Kraus, J.D., *Antennas 2nd edition*, McGraw Hill, New York, 1988
- [6] Mitra R, *Computer techniques for Electromagnetics*, Harper & Row, Washington, 1987.
- [7] Liang-Chi Shen, *Directivity and Bandwidth of Single-Band and Double-Band Yagi antennas*, IEEE Transactions on Antennas and Propagation, Nov. 1972, pp. 778-781.
- [8] David K. Cheng and C.A Chen, "Optimum Element Spacings for Yagi-Uda Arrays," IEEE Transactions on Antennas and Propagation, vol. AP-21, Sep.1973, pp. 615-623.
- [9] G.J. Burke and A. J. Poggio, "Numerical Electromagnetics Code (NEC) Method of Moments , Vol 1, pt 1: Program description-theory; Vol 1 part 2: Program description –code, Part 3 User guide," Tech Document 116, San Diego, CA, 92152, Naval Ocean Systems Centre, 1977.
- [10] G. Sato, "A Secret Story About the Yagi Antenna", *IEEE Antennas & Propagation Magazine*, Vol. 33, No. 3, pp 7-18, June 1991.
- [11] H. W. Ehrenspeck and H. Poehler, *A new Method for Obtaining Maximum Gain from Yagi Antennas*, IRE Transactions on Antennas and Propagation, Oct. 1959, pp. 379-385.
- [12] <http://www.pdscaraudio.com.au/page2.html>
- [13] Pozar, D.M, Smith Chart for Windows version 2.0, 1994.
- [14] FC Judd, *Two-metre Antenna Handbook*, Butterworth & co. Ltd., Sydney, 1980.
- [15] A.F. Inglis, *Video Engineering*, McGraw-Hill, Fair Oaks, California, 1993.

- [16] A. Netravalli and A. Lippman, *Special Issue on Digital Television. Part 1: Enabling Technologies*, IEEE Proceedings, Jun. 1995.
- [17] <http://www.zipworld.com.au/~quokka/dtvaus/index.html>
- [18] W. P. King, *Supergain Antennas and the Yagi and Circular Arrays*, IEEE Transactions on Antennas and Propagation, vol. AP-37, Feb.1989, pp.178-185.
- [19] K. Fujimoto and J. R. James, *Mobile Antenna Systems Handbook*, Artech House Inc., Geneva, 1994.
- [21] E. Bryan Carne, *Telecommunications Primer: Signals, Building Blocks, and Networks*, Prentice Hall, Upper Saddle River, New Jersey, 1995.
- [22] Cheng, David K., *Field and wave electromagnetics: 2nd ed.*, Addison-Wesley Pub. Co., 1989.
- [23] Schmitz, D., *GRAPHER: 2-D graphing system* Golden software Inc, version 1.25, 1994.

Appendix A

A.1

See ACAD file: Yagi1.dwg

See ACAD file: Yagi2.dwg

A.2

See ACAD file: Spider.dwg

Photos of antenna prototypes

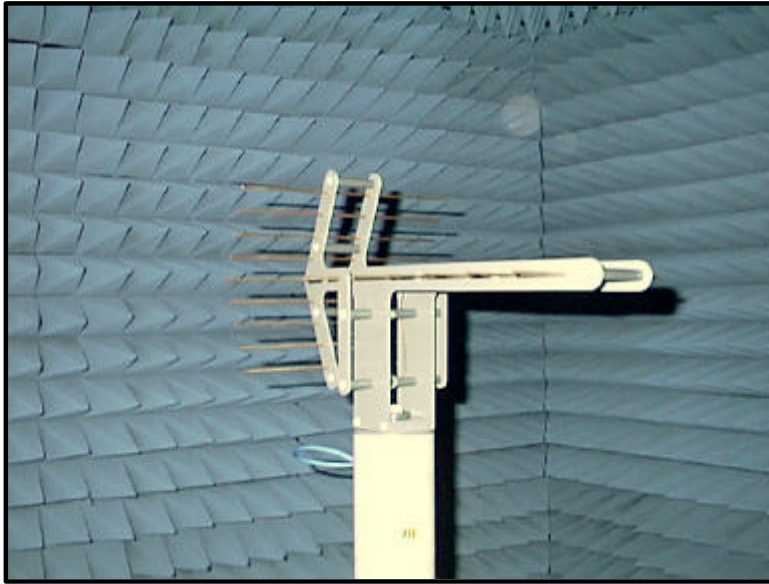


Figure A.1. Indoor Antenna - final prototype mounted on receiver turntable in anechoic chamber.

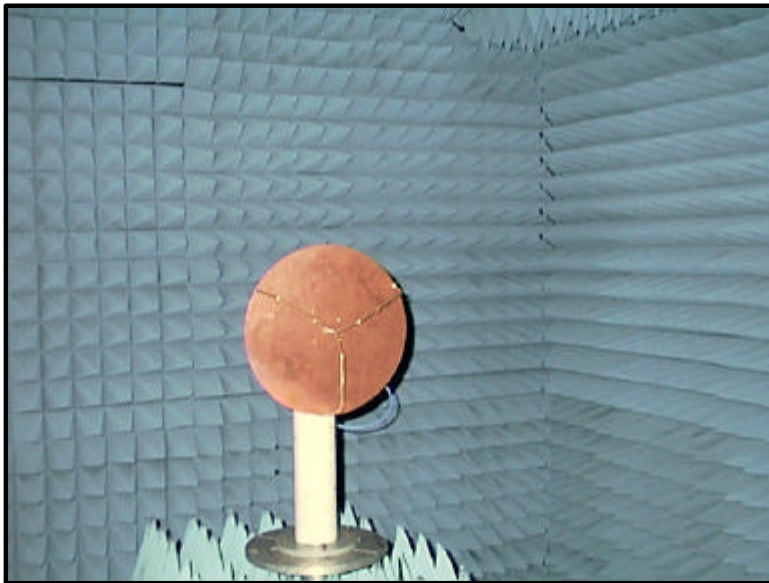


Figure A.2. Mobile Antenna – Final prototype mounted on receiver turntable in anechoic chamber.

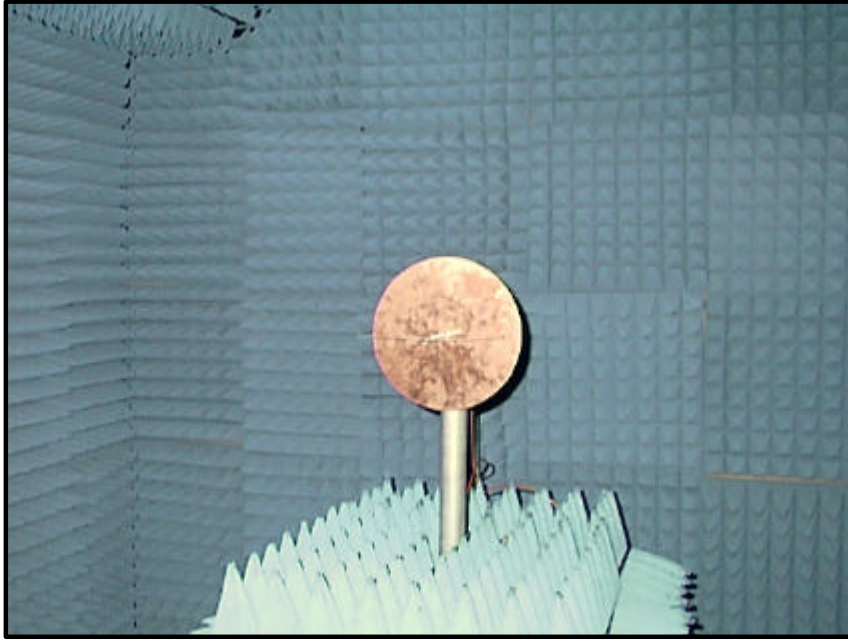


Figure A.3. Dipole transmit Antenna – mounted on transmit table of anechoic chamber.

Appendix B

B.1

Sample for NEC input data file (complete listing):

```

CM NEC Input File
CE
GW 1 13 0.00000 -0.13136 0.00000 0.00000 0.13136 0.00000 0.00111
GW 2 13 0.12878 -0.12878 0.00000 0.12878 0.12878 0.00000 0.00300
GW 3 13 0.23782 -0.10904 0.00000 0.23782 0.10904 0.00000 0.00109
GW 4 13 0.34659 -0.10904 0.00000 0.34659 0.10904 0.00000 0.00109
GE 0
FR 0 17 0 0 5.22E+02 4.00E+00 0.00E+00 0.00E+00 0.00E+00 0.00E+00
EX 0 2 7 0 1.00E+00 0.00E+00 0.00E+00 0.00E+00 0.00E+00 0.00E+00
RP 0 1 361 1401 9.00E+01 0.00E+00 1.00E+00 1.00E+00 1.00E+02 0.00E+00
RP 0 1 361 1001 9.00E+01 0.00E+00 1.00E+00 1.00E+00 0.00E+00 0.00E+00
EN

```

Sample for NEC output data file (incomplete listing):

```

*****
NUMERICAL ELECTROMAGNETICS CODE
*****

- - - - COMMENTS - - - -

NEC Input File

- - - STRUCTURE SPECIFICATION - - -

COORDINATES MUST BE INPUT IN
METERS OR BE SCALED TO METERS
BEFORE STRUCTURE INPUT IS ENDED

WIRE NO. OF FIRST
LAST TAG NO. X1 Y1 Z1 X2 Y2 Z2 RADIUS SEG. SEG.
SEG. NO. NO.
1 .00000 -.13136 .00000 .00000 .13136 .00000 .00111 13 1
13 1 .12878 -.12878 .00000 .12878 .12878 .00000 .00300 13 14
26 2 .23782 -.10904 .00000 .23782 .10904 .00000 .00109 13 27
39 3 .34659 -.10904 .00000 .34659 .10904 .00000 .00109 13 40
52 4

TOTAL SEGMENTS USED= 52 NO. SEG. IN A SYMMETRIC CELL= 52 SYMMETRY FLAG= 0

- MULTIPLE WIRE JUNCTIONS -
JUNCTION SEGMENTS (- FOR END 1, + FOR END 2)
NONE

- - - - SEGMENTATION DATA - - - -

COORDINATES IN METERS

I+ AND I- INDICATE THE SEGMENTS BEFORE AND AFTER I

SEG. COORDINATES OF SEG. CENTER SEG. ORIENTATION ANGLES WIRE CONNECTION DATA TAG
NO. X Y Z LENGTH ALPHA BETA RADIUS I- I I+ NO.
1 .00000 -.12126 .00000 .02021 .00000 90.00000 .00111 0 1 2 1
2 .00000 -.10105 .00000 .02021 .00000 90.00000 .00111 1 2 3 1
3 .00000 -.08084 .00000 .02021 .00000 90.00000 .00111 2 3 4 1
4 .00000 -.06063 .00000 .02021 .00000 90.00000 .00111 3 4 5 1
5 .00000 -.04042 .00000 .02021 .00000 90.00000 .00111 4 5 6 1
...
**** DATA CARD NO. 1 FR 0 17 0 0 5.22000E+02 4.00000E+00 .00000E+00 .00000E+00
.00000E+00 .00000E+00

```

```

***** DATA CARD NO. 2 EX 0 2 7 0 1.00000E+00 .00000E+00 .00000E+00 .00000E+00
.00000E+00 .00000E+00
***** DATA CARD NO. 3 RP 0 1 361 1401 9.00000E+01 .00000E+00 1.00000E+00 1.00000E+00
1.00000E+02 .00000E+00

```

- - - - - FREQUENCY - - - - -

FREQUENCY= 5.2200E+02 MHZ
WAVELENGTH= 5.7433E-01 METERS

APPROXIMATE INTEGRATION EMPLOYED FOR SEGMENTS MORE THAN 1.000 WAVELENGTHS APART

- - - STRUCTURE IMPEDANCE LOADING - - -

THIS STRUCTURE IS NOT LOADED

- - - ANTENNA ENVIRONMENT - - -

FREE SPACE

- - - MATRIX TIMING - - -

FILL= .033 MIN., FACTOR= .000 MIN.

- - - ANTENNA INPUT PARAMETERS - - -

TAG (MHOS)	SEG. NO.	VOLTAGE (VOLTS)		CURRENT (AMPS)		IMPEDANCE (OHMS)		ADMITTANCE REAL	
		REAL	IMAG.	REAL	IMAG.	REAL	IMAG.		
IMAG.		(WATTS)							
	2	20	1.00000E+00	.00000E+00	2.50825E-02	-6.37983E-03	3.74459E+01	9.52451E+00	2.50825E-02
			1.25412E-02						6.37983E-03

- - - CURRENTS AND LOCATION - - -

DISTANCES IN WAVELENGTHS

SEG. NO.	TAG NO.	COORD. OF SEG. CENTER			SEG. LENGTH	CURRENT (AMPS)			PHASE
		X	Y	Z		REAL	IMAG.	MAG.	
1	1	.0000	-.2111	.0000	.03519	-2.4907E-03	1.3827E-03	2.8487E-03	150.964
2	1	.0000	-.1759	.0000	.03519	-6.0862E-03	3.3721E-03	6.9579E-03	151.011
3	1	.0000	-.1408	.0000	.03519	-9.0333E-03	4.9961E-03	1.0323E-02	151.054
4	1	.0000	-.1056	.0000	.03519	-1.1435E-02	6.3154E-03	1.3063E-02	151.089
5	1	.0000	-.0704	.0000	.03519	-1.3220E-02	7.2933E-03	1.5098E-02	151.115

- - - POWER BUDGET - - -

INPUT POWER = 1.2541E-02 WATTS
RADIATED POWER= 1.2541E-02 WATTS
STRUCTURE LOSS= .0000E+00 WATTS
NETWORK LOSS = .0000E+00 WATTS
EFFICIENCY = 100.00 PERCENT

- - - RADIATION PATTERNS - - -

RANGE= 1.000000E+02 METERS
EXP(-JKR)/R= 1.00000E-02 AT PHASE -41.79 DEGREES

- - ANGLES - -		- POWER GAINS -			- - - POLARIZATION - - -			- - - E(THETA) - - -	
THETA	PHI	VERT.	HOR.	TOTAL	AXIAL	TILT	SENSE	MAGNITUDE	PHASE
DEGREES	DEGREES	DB	DB	DB	RATIO	DEG.		VOLTS/M	DEGREES
90.00	.00	-999.99	7.85	7.85	.00000	90.00	LINEAR	.00000E+00	-41.79
2.14200E-02	-49.93								
90.00	1.00	-174.50	7.85	7.85	.00000	-90.00	LINEAR	1.63373E-11	130.05
2.14124E-02	-49.95								
90.00	2.00	-168.48	7.84	7.84	.00000	-90.00	LINEAR	3.26495E-11	130.01
2.13894E-02	-49.99								
90.00	3.00	-164.97	7.83	7.83	.00000	-90.00	LINEAR	4.89115E-11	129.95
2.13511E-02	-50.05								
90.00	4.00	-162.49	7.80	7.80	.00000	-90.00	LINEAR	6.50983E-11	129.86
2.12976E-02	-50.14								

```

90.00      5.00    -160.57    7.78    7.78    .00000    -90.00  LINEAR    8.11850E-11  129.74
2.12290E-02  -50.26

```

B.2

MATLAB Programs

```

function [b]=freq_s(in_file)

%-----
% freq_s - Returns the number of frequency increment steps in the associated
%          *.nec file specified by the user
%
% last revised: by Luke Shuley 24/4/99
%-----

fid=fopen(in_file,'r');
flag = [];
b = 0;

while 1
line = fgetl(fid);
flag = sscanf(line, '%s %f %f %f %f %f %f %f %f %f');
if flag(1) == 70 & flag(2) == 82
    b = flag(4);
    break,
else
    end;
end;
fclose(fid);

%%%%%%%%%%%%%%%%%%%%%%%%%%%%%%%%%%%%%%%%%%%%%%%%%%%%%%%%%%%%%%%%%%%%%%%%

function [out_file,smith_data]=smith(file);

in_file=input('Enter name of the in file(*.NEC): ','s');
[b]=freq_s(in_file);

[smith_data]=read_z(file,b);

%outfile = input('Enter name of output file(*.DAT): ','s');
%[out_file]=write_z(smith_data,outfile);

%[max(mag)]=plot_z(complex,freq)

%%%%%%%%%%%%%%%%%%%%%%%%%%%%%%%%%%%%%%%%%%%%%%%%%%%%%%%%%%%%%%%%%%%%%%%%

function [smith_data]=read_z(file,b);

%-----
% read_z - This file reads the EAM:NEC file: 'file.out'and returns impedance data
%          for consequent use in later calculations.
%          Input par's: file(name of input file to read)
%          Output par's: Imped_data(matrix containing ordered data pairs of freq.
%          and impedance)
%
%          Rev.: 19/3/99 by Luke Shuley
%-----

fid=fopen(file,'r');          %file.out is the O/P EAM:NEC file which contains desired
data
garbage = fgetl(fid);        %assign 'garbage' to unwanted lines

line1='          - - - - - FREQUENCY - - - - -';
line2='          - - - - - ANTENNA INPUT PARAMETERS - - -';

data1=0;                      %Initialize scalar quantities

```

```

data2=0;
ix=1;
freq=[];                                %Initialize vector quantities
real_part=[];
imag_part=[];
j = sqrt(-1);

while ix <= b

%-----
% Obtain frequency data from *.out file
%-----

a=0;                                     %set marker to zero
while 1
    a = strcmp(garbage,line1);           %When line1 in output file, enter start
extracting
    if a==1                               %frequency data
        break,
    end;
    garbage=fgetl(fid);
end;

line=fgetl(fid);
line=fgetl(fid);
data1 = sscanf(line,'%s %e %s');
freq(ix) = data1(11);

%-----
% Obtain impedance data from *.out file
%-----

a=0;                                     %reset marker to zero
while 1
    a = strcmp(garbage,line2);           %When line2 in output file, enter start
extracting
    if a==1                               %impedance data
        break,
    end;
    garbage=fgetl(fid);
end;

    line=fgetl(fid);                       %Skip four lines to obtain impedance data
    line=fgetl(fid);
    line=fgetl(fid);
    line=fgetl(fid);
    data2 = sscanf(line, '%i %i %f %f %f %f %f %f');

    real_part(ix) = data2(7);               %build vector of real part of impedance.
    imag_part(ix) = data2(8);               %build vector of imaginary part of impedance.
    complex = real_part(ix) + j*imag_part(ix);

    ix=ix+1;
end;

%-----
% Collate all relevant data in smith_data
%-----

smith_data = [real_part(:),imag_part(:),freq(:)];

fclose(fid);

%%%%%%%%%%%%%%%%%%%%%%%%%%%%%%%%%%%%%%%%%%%%%%%%%%%%%%%%%%%%%%%%%%%%%%%%
function [out_file]=write_z(smith_data,outfile);

% write_z.m - Write out Imped_data matrix to a .dat file readable by
%             a windows smith chart program.
%
%             Input parameters: Imped_data(matrix containing freq. and impedance data)
%             Output parameters: outfile: output file.
%
%             last Revised:   Luke Shuley 22-3-99

```

```

ix = 1;                                     %Initialize counters
fid=fopen(outfile, 'A'); %open file designated by user 'A+' indicates an appendable
file without
                                                    %flushing contents of file.

while ix <= max(size(smith_data))

    fprintf(fid, '%6.2f', smith_data(ix,2));
    fprintf(fid, '%15.2f', smith_data(ix,3));
    fprintf(fid, '%10.i\n', smith_data(ix,1));

    ix=ix+1; %increment counter

end;
fprintf(fid, '\n');
fclose(fid); %close file
out_file=outfile; %print output filename in matlab command window..

%%%%%%%%%%%%%%%%%%%%%%%%%%%%%%%%%%%%%%%%%%%%%%%%%%%%%%%%%%%%%%%%%%%%%%%%
%
```

Appendix C

C.1

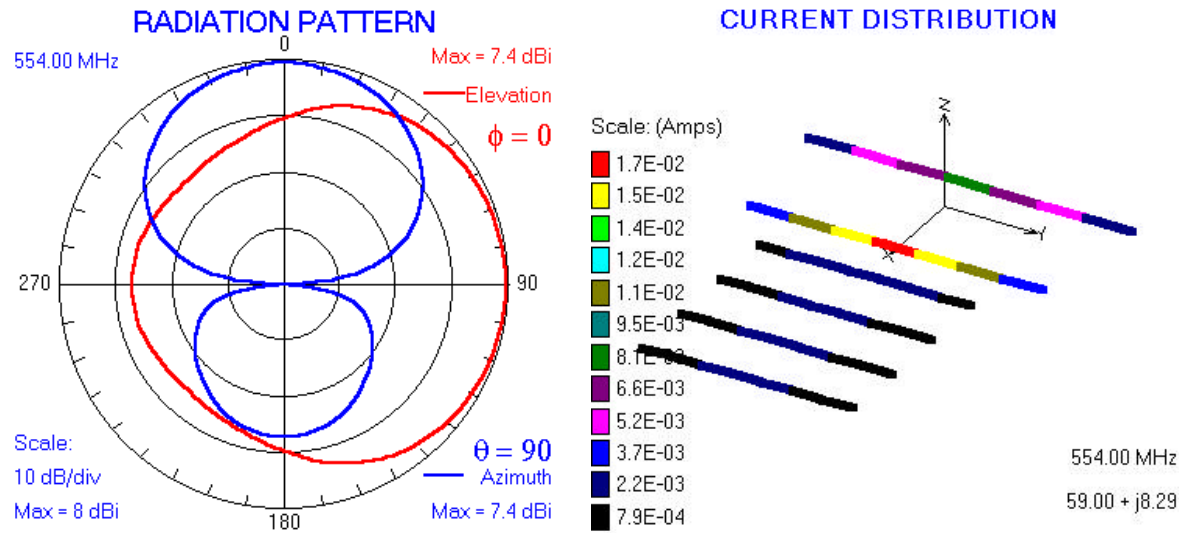


Figure C.1. Radiation Pattern and Current Distribution for Yagi_d1.out; $S_D = 0.05817m$, $S_R = 0.108m$, $L_R = 0.27618m$, $L_D = 0.18 m$, $L = 0.5 m$, $a = 0.0012m$

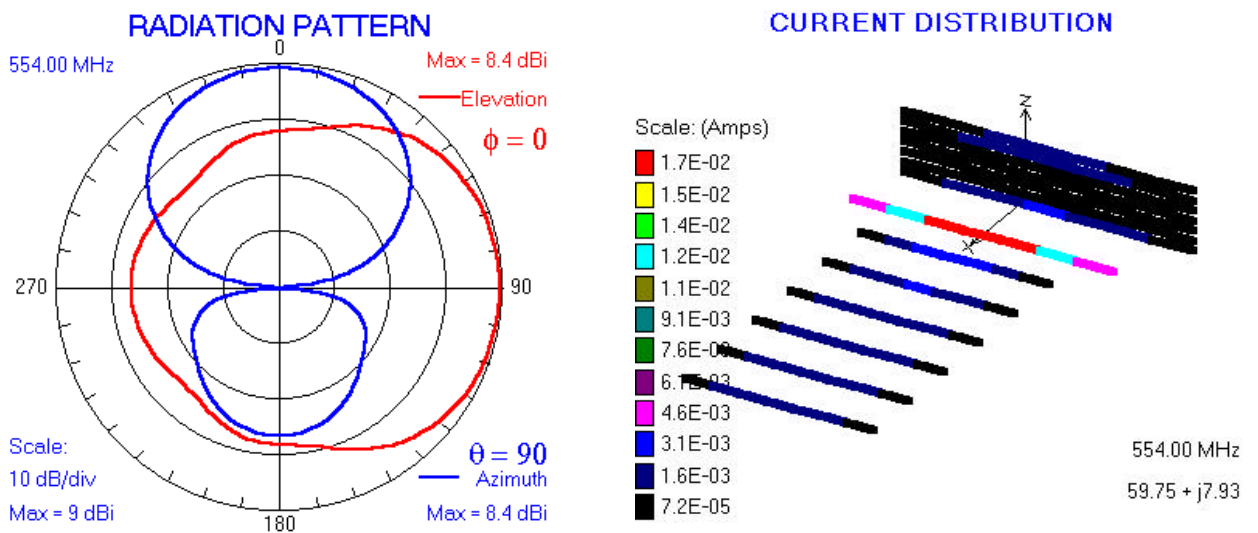


Figure C-2. Radiation Pattern and Current Distribution for Yagi_d2.out; $S_D = 0.05817m$, $S_R = 0.108m$, $L_R = 0.27618m$, $L_D = 0.18 m$, $L = 0.5 m$, $a = 0.0016m$

C.2

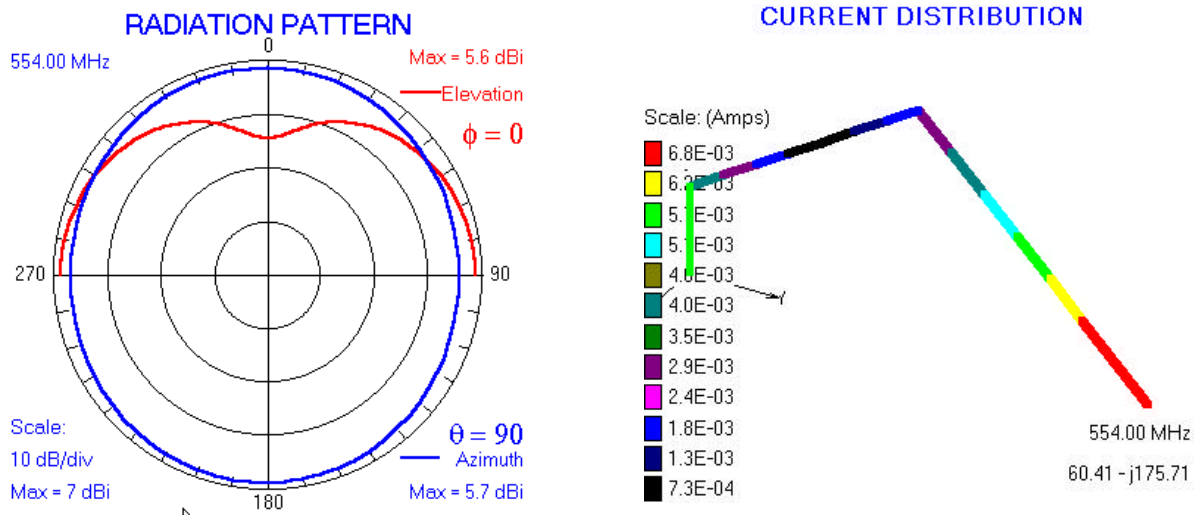


Figure C-4. Radiation Pattern and Current Distribution for $h_rhomb.out$; $L=0.16m$, $h_f=0.03m$, $h=0.08m$, $a=0.0016m$.

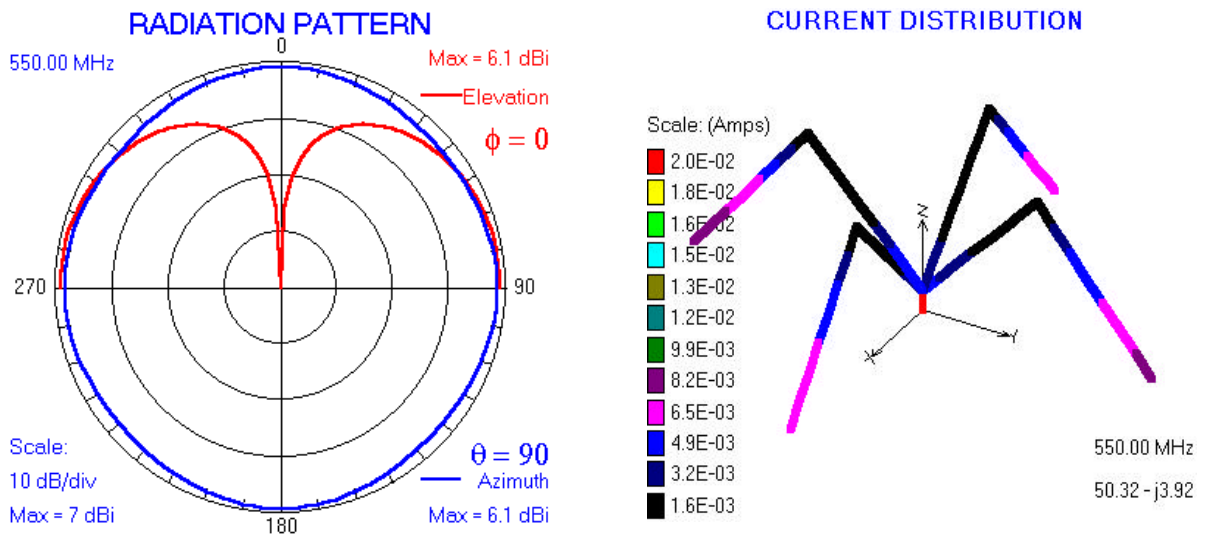


Figure C-5. Radiation Pattern and Current Distribution for $spider1.out$; $L=0.2m$, $h_f=0.017m$, $h=0.12m$, $a=0.0016m$.

Appendix D

D.1

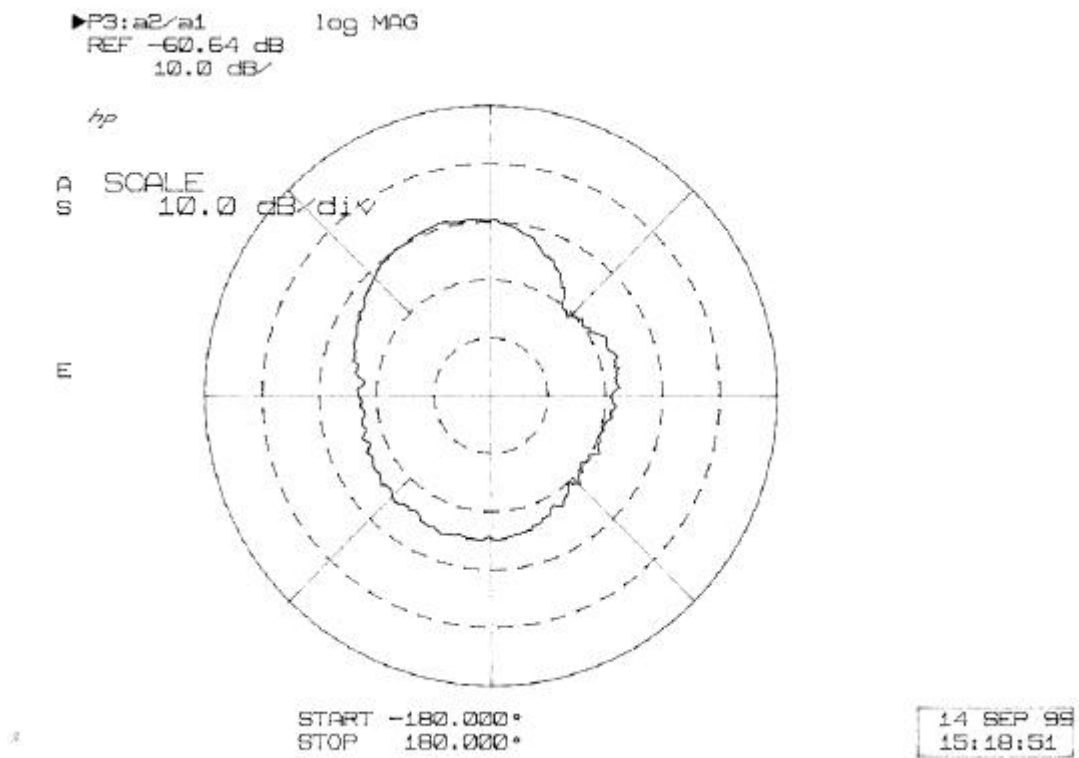


Figure D.1. Azimuth Radiation pattern of yagi_d3.nec for cross polarization

D.2

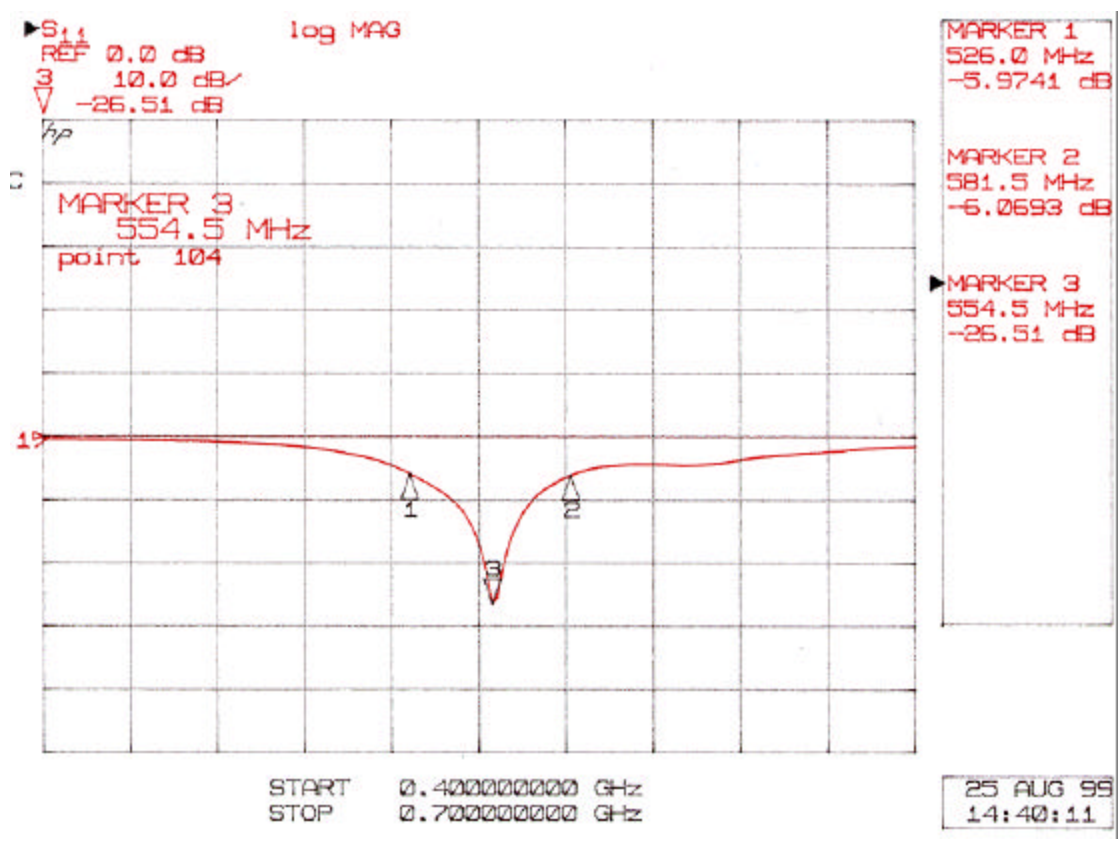


Figure D.2. Return loss of transmitter (VNA).